A Study on Surface-Emitting Lasers and Fiber Link Coupling Efficiency

Shubhankar Mishra

Department of Electrical & Computer Engineering
McGill University
Montreal, Canada

September 2021

A thesis submitted to McGill University in partial fulfillment of the requirements for the degree of Master of Science.

Abstract

Photonics in this century brings a similar revolution that electronics brought in the twentieth century. Photonics is one of the most propitious solutions to mitigate the ever-increasing demands of speed, capacity, and bandwidth for telecommunications and wireless applications. There has been a great boost in the consumption of data by applications such as video gaming, teleconferencing which requires high speed with low latency. Recently, there have been many advances within optical interconnects to achieve low loss and high data transmission rates in the data centers.

Opto-electronic integration is one of the key aspects in addressing high-speed solutions. Electrically driven Vertical Cavity Surface Emitting Lasers (VCSELs) sourced optical links are widespread in short-reach network data centers. These types of links are generally popular to use with a fiber having a multimode core for transmission. These VCSEL-multimode fiber (MMF) links provide affordable and sustainable solutions for our current data demands. These links have widespread applications in medical, industrial, and military applications such as Light Detection and Ranging (LIDAR). The common types of coupling that exist between surface-emitting lasers and the fiber that is vastly studied include with in-plane coupling or grooved fiber coupling. Effective transmission through the optical channel with high power, low loss, and good signal integrity at the photodetector requires efficient power coupling values at the transmitter side.

Increasing the power and reducing the loss are important for efficient and high-speed networks. In this thesis, we introduce Zemax as an instrument to compute the optical power coupling. We investigate and analyze the effect of misalignments on the VCSEL-MMF coupled link that can occur during optical packaging. The analysis presented in this thesis highlights the comparison between the tolerance of the Lower Order Mode (LOM)

and the Higher-Order Mode (HOM) coupling. Subsequently, we present the application of misalignments along with micro-optics to be used in the setup for spatial multiplexing in MMF and Few Mode Fiber (FMF) coupled links which can result in high data capacity solutions. Finally, we conclude the thesis by fabricating a micro-mirror on the V-grooved fiber facet setup and analyze it for potentially better power transfer which can provide a less noisy, high power solution in VCSEL array-fiber coupled links for short-reach transmission.

Résumé

La photonique de ce siècle apporte une révolution similaire à celle que l'électronique a apporté durant le vingtième siècle. La photonique est l'une des solutions les plus propices pour atténuer l'impact des demandes toujours croissantes de vitesse, de capacité et de bande passante pour les télécommunications et les applications sans fil. Il y a eu une grande poussée dans la consommation de données par des applications telles que le jeu vidéo et la téléconférence qui nécessitent une grande vitesse avec une faible latence. Récemment, il y a eu de nombreuses avancées au sein des interconnexions optiques pour obtenir de faibles pertes et des taux élevés de transmission de données dans les centres de données. L'intégration opto-électronique est l'un des aspects clés des solutions proposées à grande vitesse. Les liaisons optiques à base de laser de surface à cavité verticale (VCSEL) à commande électrique sont répandues dans les centres de données réseau à courte portée. Ce type de liens est généralement populaires à utiliser avec une fibre ayant un noyau multimode pour la transmission. Ces liens VCSEL-multimode (MMF) fournissent une solution bon marché et durable pour nos demandes actuelles de données. Ces liens ont des applications répandues dans les applications médicales, industrielles et militaires telles que la détection et la portée de lumière (LIDAR). Les types communs de couplage qui existent entre les lasers émettant de surface et la fibre qui est largement étudiée inclut le couplage de fibre bout à bout ou rainuré. Pour une transmission efficace de haute puissance, de faible perte et qui peut être facilement traitée par le canal optique au détecteur nécessite des valeurs de couplage de puissance efficaces du côté de l'émetteur. Augmenter la puissance en réduisant la perte est important pour rendre les réseaux efficaces et à grande vitesse. Dans cette thèse, nous présentons Zemax comme un instrument pour calculer le couplage de puissance optique. Nous étudions et analysons l'effet des désalignements sur le lien couplé

VCSEL-MMF qui peut se produire pendant l'encapsullation optique. L'analyse présentée dans la thèse met en évidence la comparaison entre la tolérance des modes d'ordre inférieur (LOM) et le couplage des modes d'ordre supérieur (HOM). Par la suite, nous présentons l'application de désalignements ainsi que de micro-optiques à utiliser dans la configuration pour le multiplexage spatial dans les liens couplés MMF et Few Mode Fibre (FMF) comme solutions pour haute capacité de données. Enfin, nous concluons la thèse avec une discussion de la fabrication d'un micro-miroir sur la facette de fibre V-grooved et l'analysons pour un transfert de puissance potentiel meilleur qui peut fournir une solution moins bruyante et de haute puissance pour une matrice de laser type VCSEL couplée à la fibre pour transmission à courte portée.

Acknowledgments

I would like to express my sincere gratitude to my supervisor Prof. Odile Liboiron-Ladouceur for her constant encouragement, guidance, and support throughout my program at McGill University. I am really grateful to Dr. Reza S. Nezami for his thorough advice in mode multiplexing link and his support in the micro-mirror project. I would also like to thank Shanglin Li for his help with the MATLAB verification and Lucy Wu for her help with Lumerical simulation. I would like to thank all the past and the current members of my Photonic Datacomm team for their support throughout. I would also like to thank Dr. David Rolston at Reflex Photonics and Prof. Odile for their inputs in the micro-mirror development invention. I truly thank all the professors for the outstanding coursework material, CMC for their CAD tool support and Zemax team for efficient knowledgebase and services.

I am forever indebted to my mother, brother and my girlfriend Ayesha, for believing in me. Words cannot describe how appreciative I am for everything they did and are still doing for me. It is because of their support it was possible to come to the beautiful city of Montreal for my graduate studies.

I am blessed to have my roommates Divyanshu Pandey and Shantanil Bagchi because of whom, home was never away. You guys always stood beside me and I will always cherish SSD of 1616. I can never forget my pseudo-roommates Ameya, Nikhil, Aditya, and Mostafa for all the games, food, night talks and the memories. Even in my bad days none of you lost faith in me and always encouraged me to excel. I thank all my friends and beloved ones in Montreal for their kindness and support during my study. Special thanks to my friends (Bhaukaali9) and my extended family back in India who have always requested my presence back home.

Contents

List of Figures

List of Tables

List of Acronyms

DLL	Dynamic Link Library
FMF	Few Mode Fiber
GIA	Geometrical Image Analysis
LIDAR	Light Detection and Ranging
LG	Laguerre Gaussian
LP	Linearly Polarized
MDM	Mode Division Multiplexing
MIMO	Multiple Input Multiple Output
MMF	MultiMode Fiber
NRZ	Non-Return to Zero
OOK	On-Off Keying
OSA	Optical Spectrum Analyzer
POP	Physical Optics Propagation
SDM	Space Division Multiplexing
SiPh	Silicon Photonics
SMF	Single Mode Fiber
VCSEL	Vertical Cavity Surface Emitting Laser
ZBF	Zemax Beam File
ZMM	Zemax MultiMode

Chapter 1

Introduction

1.1 Motivation

The inherent advantages of photonics over electronics are low loss transmission, immunity from electromagnetic interference, and most importantly very high data transmission. Photonics is the branch of physical science that deals with the manipulation of information represented by optical signals. It typically involves the generation, modulation, transmission, switching, amplification, signal processing, and detection of light. High data rate demands and internet traffic have continued to grow heavily during recent times. Rise in the applications such as video gaming/conferencing, cloud data storage, etc., have only soared the demand for power and speed further. Optical interconnects are required to efficiently transmit data from one part to the other using light. Figure 1.1 shows the traffic data from 2017 projected up to 2022. The connected devices to the Internet Protocol in 2022 is much more than the projected global population in 2022 [1].

Figure 1.2 shows the increase in data transmission or the fiber capacity utilisation since 1970 for long haul networks. The capacity of 140 Mbits/sec was prominent in the 1980s for the Plesiochronous Digital Hierarchy (PDH) technology when the single mode fibers started to be deployed. Synchronous Digital Hierarchy (SDH) soon arrived in the 1990s offering advantages over the PDH such as optical interfacing, flexible, and synchronous structures.

The invention of fiber amplifiers made Wavelength Division Multiplexing (WDM) possible which, along with coherent detection further improved the transmission capacity. The plot

Fig. 1.1: Projected IP traffic growth by the year globally [1].

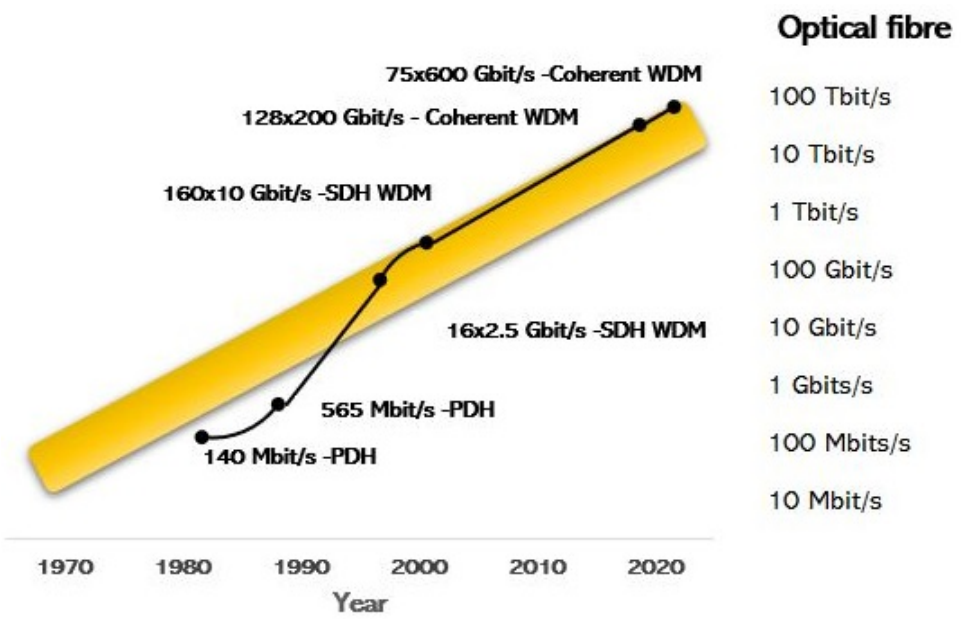

Fig. 1.2: Transmission capacity of optical fiber (trend over the years) [2].

shows that the transmission capacity is doubling every year [2]. As the system capacity increases, the speed of the networking interfaces should also advance to limit the complexity of the network. Improving interfacing speed is one of the most important aspects in short reach communication links. In [3], the interface rates for a variety of networking equipment versus the optical system, cross connects, and the router is discussed. Before the 21st century, the cross connects and routers used lower rates than those available for transmission. It is also shown that since the 2000s, the rates for transmission, cross connects, and the routing speed amalgamated and continued to grow. From the speed of 10 Gbps in the beginning of the 21st century, the future extrapolation of the data suggest that the speeds for such networks could touch 1 Tbps by the 2020s.

With this rapid and imminent growth, it is of utmost importance that we also focus on minimising the power consumption as well. High capacity networks having efficient transmission is the first step in this direction. Laser to fiber links form the backbone of the transmitter in the communication channel. Efficient coupling of power from the laser plays a vital role in increasing data transmission with respect to the energy consumed. Data encoded with different modulation formats and multiplexing techniques also prove advantageous. In this work, we study the power coupling efficiency of laser to fiber setup with a focus on deploying multiplexing solutions for such links.

1.2 Thesis Objective and Outline

This thesis presents the use of Zemax as a tool or method to design and mimic a free space laser-fiber coupled setup. This coupled setup using Zemax helps us get better understanding of such systems where precise control over selective modes in the laser-fiber setup is difficult to achieve and analyse for different applications that may involve studying quantitative sensitivity to misalignment in the packaging. It can be achieved by observing the effect of misalignment on coupling efficiency in such setup and how it can be utilised for different applications. One such application we can use the Zemax setup to study is Mode Division Multiplexing (MDM). We deploy micro-optics (lens) and misalignment for Mode Division Multiplexing (MDM) applications. This setup promises more data on different channels without increase in the interference between modes. Finally, we focus on deploying a gold

coated mirror and decentralisation for the arrayed VCSEL to grooved fiber coupling for packaged transceivers. The modification helps the already existing conventional industry standard structure to be more power efficient. This thesis consists of seven chapters. The outline of the thesis is as follows:

- Chapter 1 is the introduction and motivation for the work.
- Chapter 2 reviews the basics and gives a general background of the VCSELs, MMF, and mode theory utilised before focusing on the development of the short reach network capacities.
- Chapter 3 introduces the use and features of commercial tool, OpticStudio by Zemax for the calculation and analysis of laser-to-multimode fiber coupling. Two methods and their usefulness have been discussed.The sequential method has been used as the tool throughout the thesis to calculate the power coupling efficiency.
- Chapter 4 discusses the use of Zemax's Physical Optics to study the effects of misalignment in mode-to-mode free space coupling of a VCSEL and an MMF link.
- Chapter 5 demonstrates the application of chapter 4 for a mode division/spatial division multiplexing (MDM/SDM), based on launch selective coupling in a VCSEL-MMF transmission setup. The application of MDM is also discussed for laser-Few Mode Fiber (FMF) links.
- Chapter 6 presents the coupling study of a conventional laser and a 45° reflecting type fiber link. The design and simulation of the modified structure having better power coupling efficiency are included. Fabrication and the initial test measurements of the fabricated prototype are also discussed. I did the simulation work on the design and helped in brainstorming the fabrication ideas. The fabrication is from SiJ Technologies, and the setup measurements were performed by my colleague Dr. Reza Nezami, a postdoctoral student in our research team at McGill, along with Dr. David Rolston and other fellow colleagues at Reflex Photonics (now Smiths Interconnect) at their facility in Kirkland, Canada. All the results and images presented in this chapter are with permissions from Reflex Photonics (Smiths Interconnect).

The concept in chapter 6 was submitted to the United States Patent and Trademark Office (USPTO):

US Application Number- 63/018639, *Filing Date*- 05/01/2020, "SYSTEMS AND METHODS FOR COUPLING LIGHT", *Inventors*- David Rolston, Shubhankar Mishra, Mohammadreza Sanadgol Nezami, and Shanglin Li.

- Chapter 7 summarises the thesis and discusses the future scope.

The findings in this thesis have influenced the work by PhD candidate Shanglin Li and can be find in the following peer-reviewed journal article:

* Shanglin Li, Mohammadreza Sanadgol Nezami, *ShubhankarMishra*, Odile Liboiron-Ladouceur "Spectral-dependent electronic-photonic modeling of high-speed VCSEL-MMF links for optimized launch conditions" in OSA Optics Express, vol. 29, no. 2, page 2738-2756 (2021).

Chapter 2

Background

2.1 Introduction

In this chapter, we commence with the theory of optical communication links and their modules. We discuss the basics and fundamentals of the short reach transmission network with due focus on the VCSEL-MMF. We present in brief the theory of VCSELs and MMF and the role they play in data communication. We also discuss about the development of such interconnect links and some works that relate to it. We conclude with a short discussion on new advancements in VCSEL technology for different applications.

2.2 Fiber Optic Communication Links

The block diagram of a basic fiber optic communication link with a single channel that transmits and receives digital information is presented in figure 2.1. At the transmitter side, it has a laser diode (LD) where electrical data is directly modulated on the optical stream for transmission. Then, we have the optical fiber which may be SMF or MMF with splices and connections along the way to the receiver for long haul connections or data centers, respectively. At the receiver end, there is a photodetector (PD) with the necessary circuitry for equalization and signal processing. At the receiver end, the optical data is then recovered to form the original transmitted electrical data stream [4]. Bit Error Rate (BER) is an important parameter to assess the transmission link performance that is computed at

the receiver decision part. BER is a benchmark value that conveys the ratio of incorrectly decoded bits. Values of BER are generally desirable in the order of 10^{-12}. Additionally, in the long haul network links we have additional amplifiers along the data route for compensating the optical losses over long distances.

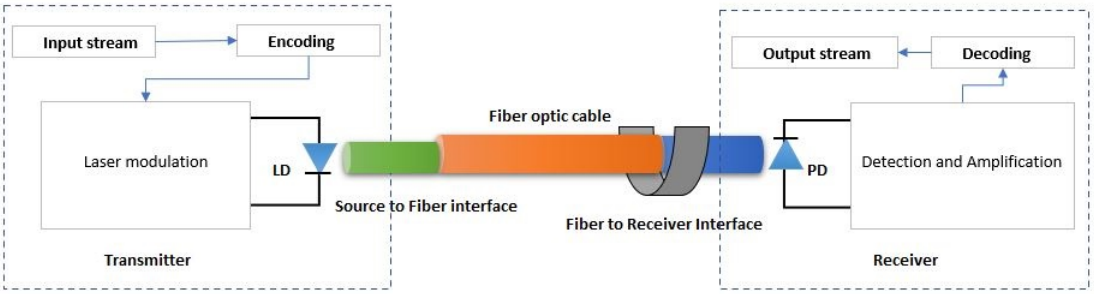

Fig. 2.1: Point to point optical fiber communication link.

2.3 VCSEL-Fiber Theory

2.3.1 VCSELs

VCSEL, or Vertical Cavity Surface Emitting Lasers, as the name suggests emit light vertically from the top perpendicular to the surface, unlike conventional edge emitting lasers [5]. The active area structure of the VCSEL is shown in figure 2.2.

The gain area (Quantum Well (QW)) is confined between two reflectors or mirrors with opposite doping which produces the lasing action. The gain area can be as small as a few microns for output powers of 0.5 mW up to a hundred micron for powers as high as 100 mW for multimode devices [6]. VCSELs are deployed in different applications commercially, for example lasers with long wavelength find usage in optical fiber communication, biomedical photonics, etc. [7],[8]. Lasers operating at short wavelengths help in lithography, lighting displays, and projectors [9],[10],[11]. VCSELs emitting wavelength in the range of 850-1040 nm generally find their use in the area of optical interconnects [12],[13].

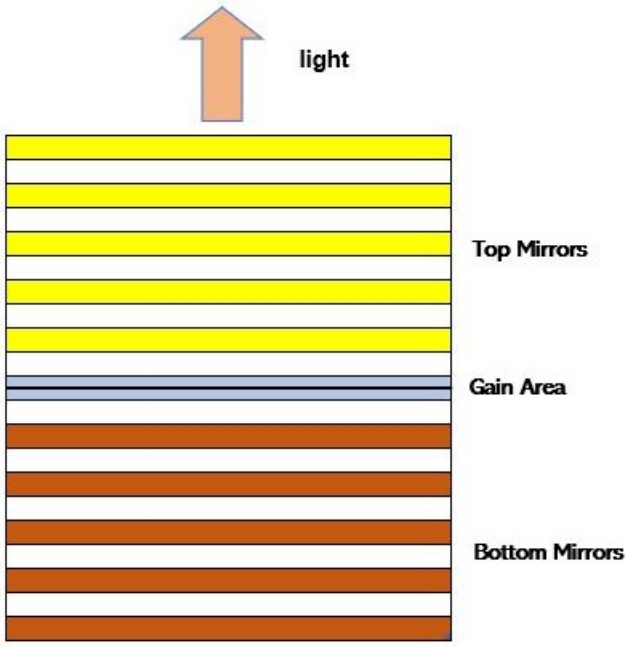

Fig. 2.2: Active area structure with reflective mirrors [6].

2.3.2 Optical Fibers (SMF and MMF)

Optical fibers are used to transmit light over short or long haul with higher data rates than their electrical counterparts like cables. There are generally two prominent classifications namely, single mode fibers and multi mode fibers. Figure 2.3 shows the comparison of an MMF and an SMF. The cladding has a lower Refractive Index (RI) than the core and they work on the principle of Total Internal Reflection (TIR) [14]. The SMF, as evident by its name supports a single mode (the fundamental mode) and the MMF can support several of Higher Order Modes (HOM) as well. The modes in a fiber can be calculated by solving the characteristic equation. The fibers are weakly guiding so degeneracy (same propagation constant) occurs and the concept of Linearly Polarised (LP) modes is established [15]. As the optical fiber is weakly guiding, a few modes that combine or have identical propagation constants form a mode group [16]. It is shown in [17] that most of the power propagating in optical fiber is confined to the first few LOM and is not uniformly distributed to all the permissible modes. Thus, Mode Power Distribution (MPD) is non uniform in semiconductor

laser-fiber setup.

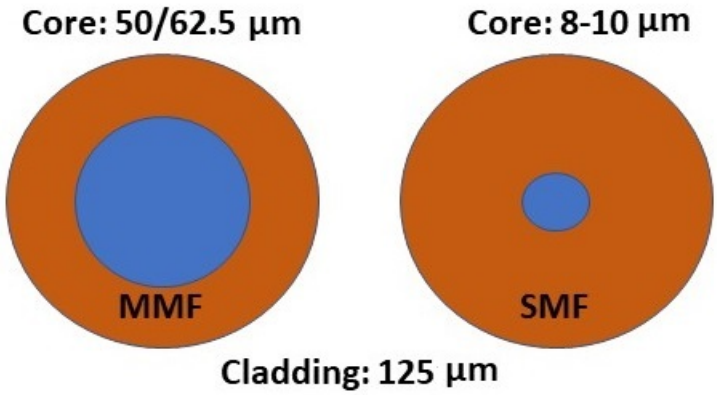

Fig. 2.3: Representation of a multimode fiber and single mode fiber.

2.3.3 Modes in a Fiber

In the previous section, we defined the types of fibers and the modes they can support. A potential path that a light ray can take inside the fiber is termed as a mode. SMF supports only a single ray (beam) that travels through the center. A MMF on the other hand can support a large number of guided modes. The lower-order modes and the higher-order modes tend to limit light spatially near the core and around core-cladding interface respectively [18][19]. We can estimate the number of modes supported by a fiber using equation (2.1) where M denotes the number of modes and V is the normalised optical frequency.

$$M = \frac{V^2}{2} \tag{2.1}$$

The V number is a dimensionless quantity that is normalised to the guiding properties of the fiber as shown in equation (2.2). The V number depends on the fiber core radius a, free space wavelength λ, and the numerical aperture (NA) of the fiber [20].

$$V = \frac{2aNA\pi}{\lambda} \tag{2.2}$$

Equation (2.3) provides the values of the NA where n_{core} is the refractive index of the core and n_{clad} is the refractive index of the cladding.

$$NA = \sqrt{{n_{core}}^2 - {n_{clad}}^2} \tag{2.3}$$

A fiber is termed as a SMF if the V-number is less than 2.405, which signifies that only the fundamental mode exists. If the core of the fiber is just large enough to support a few modes in addition to the fundamental mode, this type of fiber is referred to as a few mode fiber (FMF). A Few Mode Fiber (FMF) is also a great candidate to replace the MMF for MDM applications [21]. The benefit it offers over the MMF include noise mitigation, low MIMO processing complexity among many others [22]. FMF-laser links as an application of MDM is discussed in chapter 5.

2.4 State-of-the-Art Review

In this section, we will briefly present the advancement in the area of VCSEL-based communication links over the years until recently. VCSELs have been in the market since the late 1970s. In the past two decades they have become famous as they offer cost effective and high speed data links. Authors in [23] presented in 2002 optimized VCSEL aperture sizes to achieve over 10 Gbps transmission over Graded Index (GI-50) MMF. Results in 2012 indicated in [24] showed that their VCSEL and PD fared well from the perspective of speed and heat dissipation and produced error free links at bit rates over 25 Gbps over different ranges of length and temperatures of operation. This provided the understanding that such links offered solutions to next generation of multimode optical fiber interconnects.

The work in [25] presented 850 nm multimode VCSEL produced performance sufficient for error free transmission over 100 m of an OM3 fiber at 25.78 Gbps over a range of temperatures. In [26], VCSELs capable of direct modulation over 40 Gbps were useful for the optical interconnect standards. This work from 2013 utilised a refined high speed design for VCSELs based on Galium Arsenide (GaAs) having 28 GHz modulation bandwidth for error-free operation at 47 Gbps. In 2013 again, a chip to chip optical link demonstrated the highest serial bit rate standing at 56.1 Gbps for NRZ modulated VCSEL. In [27] we observed

that NRZ modulated links offer convenient and practical option to cater the high serial data rates without the use of complex encoding or modulation format which require further equalisation at the receiver end, and also may utilise pre-compensation at the transmitter side of the link .

The 2014 review article [28] by *Tatum* shares the evolution of the deployment of 850 nm based VCSELs for data transmission rates that increased over time from 10 Gbps to 25 Gbps to 56 Gbps. It was further highlighted that for VCSEL-MMF based links to compete with Silicon Photonics (SiPh), improvement in several factors including power consumption, cost multimode interconnection, and cost effective optical packaging was imminent. Increased data transmission capacity is required to support the growth and innovation in the optical communications. Reference [29] stressed on the application of other mechanisms to improve the data throughput such as the utilisation of SDM for free space data communication at data rates of around 28 Gbps for On-Off Keying (OOK) modulation format. To achieve bit rates over 56 Gbps and above, spectral efficient advanced modulation formats are required. In [30], PAM-8 modulation format was used to achieve higher spectral efficiency to provide data rate above 100 Gbps per lane with a VCSEL and OM3 MMF to achieve bit rates ranging from 90 Gbps for 125 m of fiber to 108 Gbps over 25 m of the fiber. The review from 2014 in [28] highlighted the evolution of data transmission rates. Previously, results for 56 Gbps was shown for complex modulation formats such as PAM-4 and PAM-8 which can be upgraded to 56 Gbps for NRZ. To achieve the transceiver rates of over 400 Gbps, the need for spatial and spectral multiplexing for VCSEL based links was underlined in [31]. Reference [32] in 2020 reviews the challenges that the next generation of 850 nm based VCSEL-MMF based data links face to achieve up to 100 Gbps per channel transmission.

2.4.1 MDM for High Capacity Links

As reported and discussed above, modulation formats and multiplexing are fundamental for next generation of such links. Mode division multiplexing (MDM) increases the capacity of the next generation of optical interconnects. Vertical cavity surface-emitting lasers (VCSELs) coupled into multi-mode fiber (MMF) is widely adopted as a cost-effective solution for short and mid-reach high-speed data transmission. In MMF, the signal transmitted over several

modes leads to dispersion and thus, Inter-Symbol Interferences (ISI) at the receiver [33]. Few-mode VCSELs can selectively stimulate lower order modes (LOM) and higher order modes (HOM) in a multimode fiber by controlling the launching condition mitigating intermodal dispersion and form the basis of spatial multiplexing. Current works show that few mode VCSELs can be controlled to emit only certain desired modes in MDM systems [34],[35]. In [36], it was shown that MDM can be achieved along with Wavelength Division Multiplexing (WDM) for increasing the bandwidth of the MMF by Spatial Light Modulator controlled VCSELs. In [37], MDM is achieved in a VCSEL-MMF setup by controlling the emission of desired modes from the VCSEL using diffraction elements, and combining them onto the MMF. The concept of beam profile control to generate inputs is also referenced in [38]. In [39], *Xie et al.* showed that ultrathin flat optical structures (Metasurfaces) also presents a powerful technique to maneuver the beam profiles with high efficiency *i.e.*, emission of desired modes. Later in this work, we show that the beam profiling discussed above can be achieved with the help micro-optics for a FMF setup that can be applied to such links effectively . This allows us to selectively generate, couple, and transmit the data on desired modes using MDM to achieve high capacity. These links with effective receiver modules can be utilised to form the backbone of Multiple Input Multiple Output (MIMO) systems where each of the MDM signals are considered as multiple inputs to the system carrying information.

Chapter 3

Zemax OpticStudio for Coupling Study

3.1 Introduction

In this chapter, we introduce the methodology exploiting CAD tool OpticStudio (by Zemax [40]) which we use in the subsequent chapters. Zemax Opticstudio is an optical design software used by optical designers all over the world to design, visualize, and analyze optical systems. It offers various options to play with different parameters to configure sources, detectors and optical devices such as lens, mirrors, prisms including complex optical elements. In this work Zemax's sequential mode is used to quantify the coupling efficiencies of a source (laser) to fiber link with or without micro-optics. The sequential mode allows the use of wavefront propagation (POP) through the defined surfaces in the system. This chapter forms the basis of the methodology used for further chapters. We introduce the two different approaches which are generally used for computing coupling efficiencies namely the Ray tracing based model and the Physical Optics based model. OpticStudio can be used to compute coupling into a Single Mode Fiber (SMF) or an MMF. The discussion here is limited to MMF.

3.2 Ray Tracing for Coupling Efficiency

The ray based tracing for multimode fiber efficiency calculation is achieved with the aid of Geometric Image Analysis (GIA) in Opticstudio. It uses geometric rays to propagate light through the system from the source to the fiber surface. A more detailed explanation for this section is available on Zemax Knowledgebase [41].

3.2.1 Description of Zemax Geometric Image Analysis (GIA)

For showing the concept of ray tracing in GIA, we assume a simple setup as shown in figure 3.1.

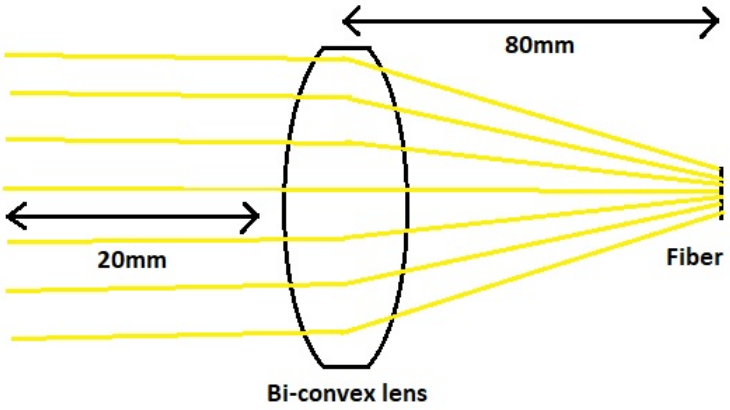

Fig. 3.1: GIA setup for ray tracing to a fiber.

As we operate in the sequential mode, the multimode fiber is the last surface on which we compute the coupling efficiency. The fiber has a core of 0.09 mm in diameter and a Numerical Aperture (NA) of 0.2. These two parameters are one of the few parameters required in the GIA dock (task bar) to define the incoming rays to the fiber for coupling. A conventional biconvex lens (focussing lens) has a focal length of 90 mm, an aperture of 25 mm, and a thickness of 15 mm and made of N-BK7 material. In this work, we use N-BK7 material (glass) for our lens material as it is low cost and works well in the infrared region around 850 nm, the wavelength at which the VCSELs work in industrial applications [42]. The transmission function of N-BK7 is high (over 90%) even after several ionising radiation

tests which proves its strength for various applications [43].

3.2.2 Initial Observations-GIA

Figure 3.2 shows the computed efficiency at the fiber surface for an optical source emitting at 850 nm. The coupling value is very low with 2.2% for an input optical power of 10 mW. The poor coupling efficiency reflects non-optimum initial parameters. To improve the ray coupling to fiber, it is important to optimize the parameters (lens material, shape, radius, spacing, etc.) of the setup. For example, in the GIA setup, the spacing between the lens and the fiber is assumed to be a variable on which the optimising function can operate.

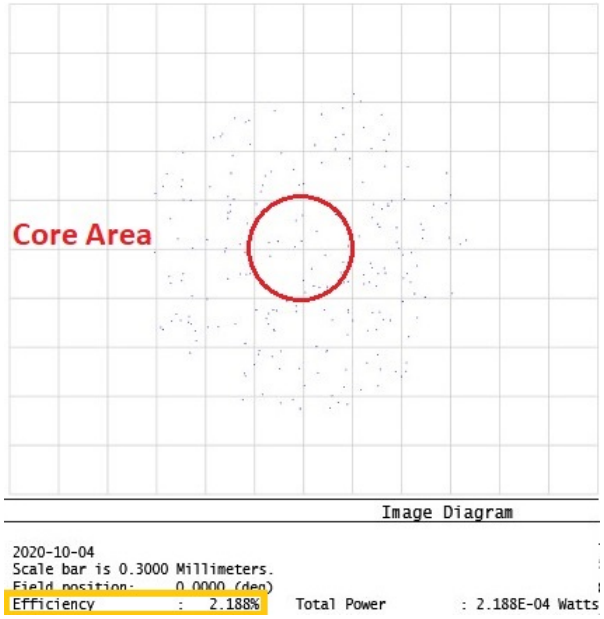

Fig. 3.2: Coupling efficiency computed at the fiber surface.

Figure 3.3 shows the computed efficiency with the spacing value changed from 80 mm to 85 mm using the IMAE operand. The IMAE optimization operand is used to obtain the fractional efficiency of the system for the propagation of light from the object plane to a surface of interest [41]. We observe a great improvement in the coupling from 2% to 55% with the lens-fiber distance variable optimized. It is also worth noting that it is further

possible to enhance the coupling by varying other parameters of the setup.

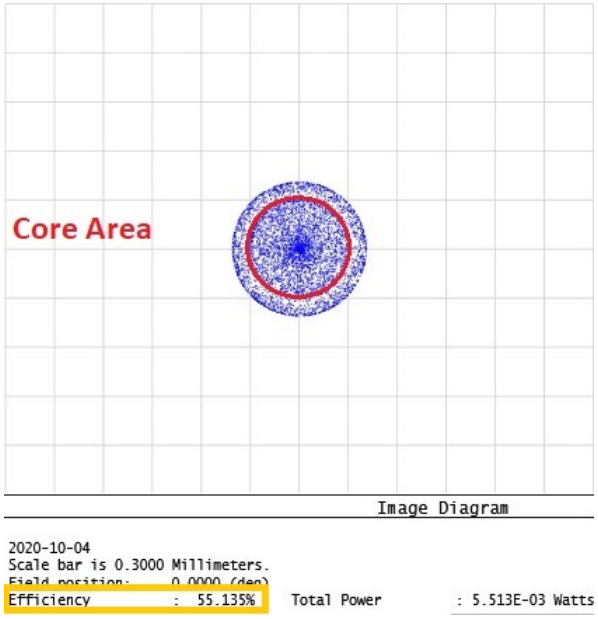

Fig. 3.3: Optimised coupling efficiency at the fiber surface.

3.2.3 Conclusion

The Geometric Image Analysis (GIA) simulation method from OpticStudio computed the VCSEL to MMF coupling efficiency through a lens. Different types of ray (Gaussian, Apodised) can be used to evaluate similar setups. The analysis can also be done for different materials of the fiber core. It is also possible to include parameters impacting coupling not restricted to scattering, fresnel losses, and glass absorption, etc. in the lens data dock. Mode group information and power distribution in each fiber mode needed to determine for different applications is not available in GIA.

3.3 Physical Optics Propagation for Coupling Efficiency

Physical Optics Propagation (POP) in Zemax uses wavefront propagation as opposed to geometric rays. Unlike rays, the wavefronts propagate and interfere with each other either

coherently or incoherently, and diffract. Hence, POP is more useful to obtain a good approximation when calculating modal coupling efficiency. It is worth noting that if modal/beam information is not required, POP allows us to traverse a part of the optical setup using rays. The coupling efficiency (PCE) in POP is the product of system efficiency (fiber receiving part of the beam) and receiver efficiency (conversion of free space mode to fiber mode). In this section, we discuss the system used in POP with the input mode of the laser source and the output mode of the fiber.

3.3.1 Laser Source Input Modes

Figure 3.4 shows a surface emitting laser beam from a VCSEL having a circular gain region and a circular aperture. The optical modes generated by the VCSEL can be approximated as Laguerre Gaussian (LG) modes [44]. The LG modes are used as the free space modes outside the laser cavity and as the input to our optical system. The electric field E_{pl} of the LG modes can be described by equation (3.1) below which is the solution for a plane wave solving the Hemholtz equation.

$$\begin{aligned} E_{pl}(r,\phi,z) =& \sqrt{\frac{2p!}{\pi(p+|l|)!}}\frac{1}{w(z)}\Big[\frac{r\sqrt{2}}{w(z)}\Big]^{|l|}\exp\Big(\frac{r^2}{w^2(z)}\Big)L_p^{|l|}\Big(\frac{2r^2}{w^2(z)}\Big) \\ & \times\exp\Big(-ik\frac{r^2}{2R(z)}\Big)e^{il\phi}\exp\Big[i(2p+|l|+1)\tan^{-1}\Big(\frac{z}{z_0}\Big)\Big]e^{-ikz} \end{aligned} \tag{3.1}$$

The LG modes have circular symmetry and can be represented in terms of Laguerre polynomial $L_p^{|l|}$, where z_0 is the Rayleigh range, w_0 is the beam waist, $w(z)$ and $R(z)$ are the values of beam width and wavefront radius of curvature, l and p are the orbital angular momentum (OAM) and radial index, respectively [19],[45],[46]. In OpticStudio, the LG modes are defined in the Dynamic Link Library (DLL) by the order of the mode (radial and azimuthal), the beam waist, and the rotation (even or odd). It is also possible to define every mode independently or as a combination of modes by generating a Zemax Beam File (ZBF) or a Zemax MultiMode (ZMM) file, respectively. The POP features also allow to define various types of beams such as Gaussian waist beam, astigmatic Gaussian beams, etc. For this work, we use the LG beams generated from the laguerre.dll file in Zemax.

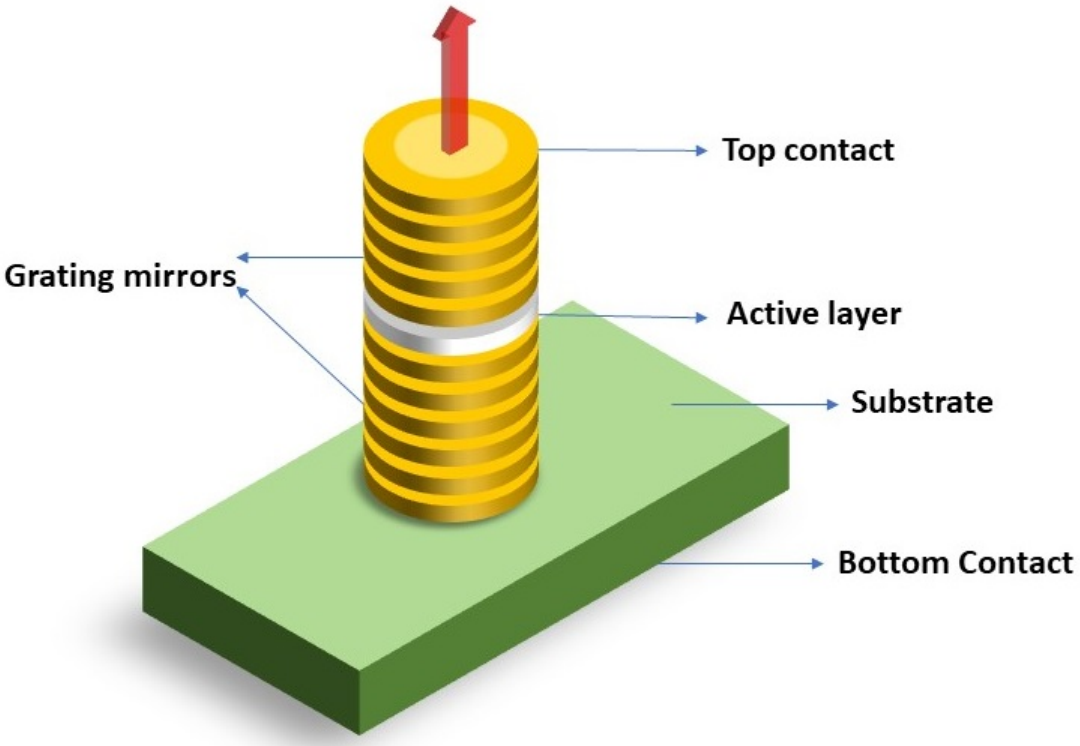

Fig. 3.4: VCSEL beam from a circular gain aperture.

Figure 3.5 shows a LG00 even mode generated in Zemax OpticStudio with a Gaussian beam waist of 3 μm. The wavelength used is 850 nm with air as the propagation medium. The colour bar profile shows the intensity of the light which is a function of various parameters such as the input power, position of the image plane and more.

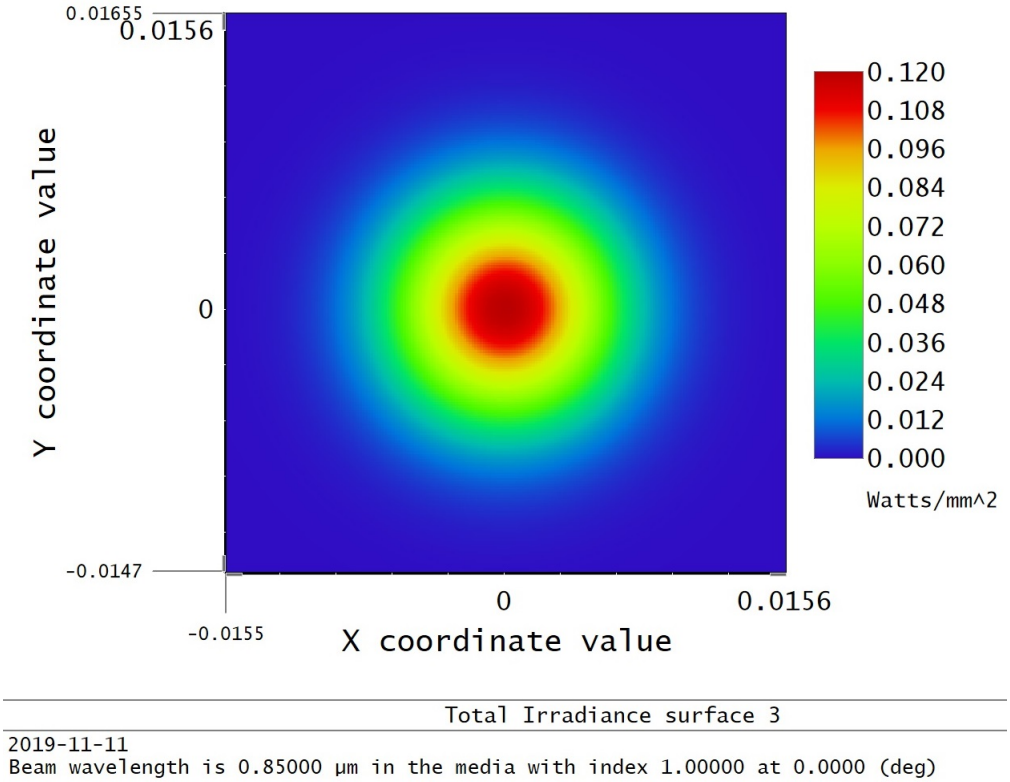

Fig. 3.5: LG00 even mode profile in Zemax with the x-axis and y-axis representing the distance in nanometer.

3.3.2 Fiber Output Modes

Zemax provides different built-in files and formats to use as the fiber modes are similar to the input modes. For example, it is also possible to use the input mode as the output mode for self-coupling value check in a free space or in a complex system. The output mode

(fiber modes) for this work has been generated using Lumerical MODE solutions for the coupling analysis. Lumerical MODE solutions is a simulation tools that numerically solves Maxwell's equation for a given structure. The Zemax-Lumerical interoperability license is used to export the electric field profile data at the fiber surface from MODE solutions in a ZBF file format which is then used in the Zemax optical system. Figure 3.6 below shows the fiber LP21a mode profile imported into Zemax from MODE using the beam file viewer setting in OpticStudio. Lumerical MODE uses a Graded Index (GI) MMF with core and cladding index of 1.45 and 1.43, respectively. MODE solutions calculates the optical modes in the fiber at a wavelength of 850 nm. The fiber modes in MODE can be combined to give LP modes. The first few mode groups are sufficient in our analysis.

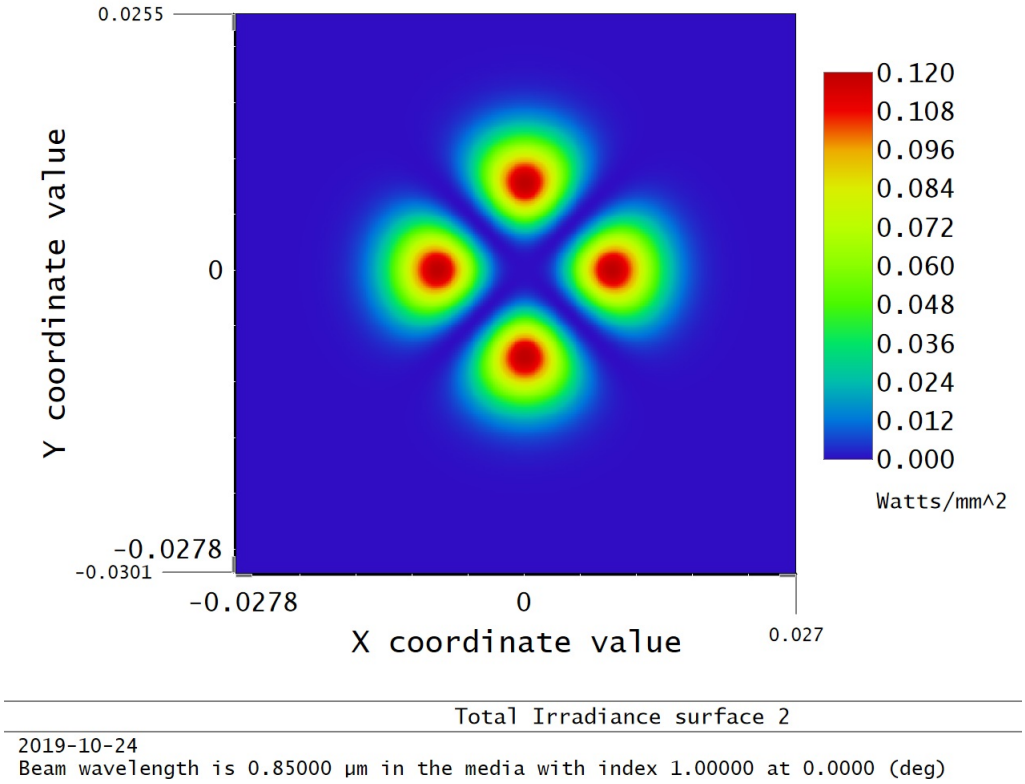

Fig. 3.6: LP21a mode profile in Zemax with the x-axis and y-axis representing the distance in nanometer (imported from MODE).

3.4 Fiber Coupling Calculation

The system coupling efficiency is determined by the light intensity incident to the fiber surface. As the fiber core is larger than the beam waist, the small distance gap between the laser aperture and the fiber surface does not affect coupling efficiency. The fiber coupling efficiency, on the other hand, is defined as the normalised overlap integral of the incoming optical wave to the fiber surface and the fiber mode field. Equation (3.2) below shows the fiber coupling calculation where $F(x, y)$ is the electric field amplitude of the fiber mode and $B(x, y)$ is the electric field amplitude of the optical input signal at the surface of the fiber. We calculate the overall coupling efficiency T which gives a value of unity if the input mode and output mode match perfectly in both amplitude and phase. As an optical mode propagates, its beam may experience losses through scattering and absorption limiting the total optical power transfer. In chapters 5 and 6, we use micro-optics to reduce the beam divergence and obtain better focus which increases the receiving fiber coupling efficiency which consequently increases the total coupling.

$$T = \frac{|\int\int F(x,y)B'(x,y)dxdy|^2}{\int\int F(x,y)F'(x,y)dxdy \int\int B(x,y)B'(x,y)dxdy} \tag{3.2}$$

3.5 Lens Data Settings

We design our optical system in subsequent chapters using the parameters shown below in figure 3.7. The Zemax lens data dock allows to define several parameters such as its surfaces, dimensions, materials, coatings, curvatures, rotations, etc. These settings allow us to investigate the impact of various lens on the VCSEL-MMF mode coupling efficient.

In chapter 4, the performance impact of misalignments of the lens is investigated by modifying the lens data. Figure 3.8 shows a basic setup with angular misalignment between the source and image plane.

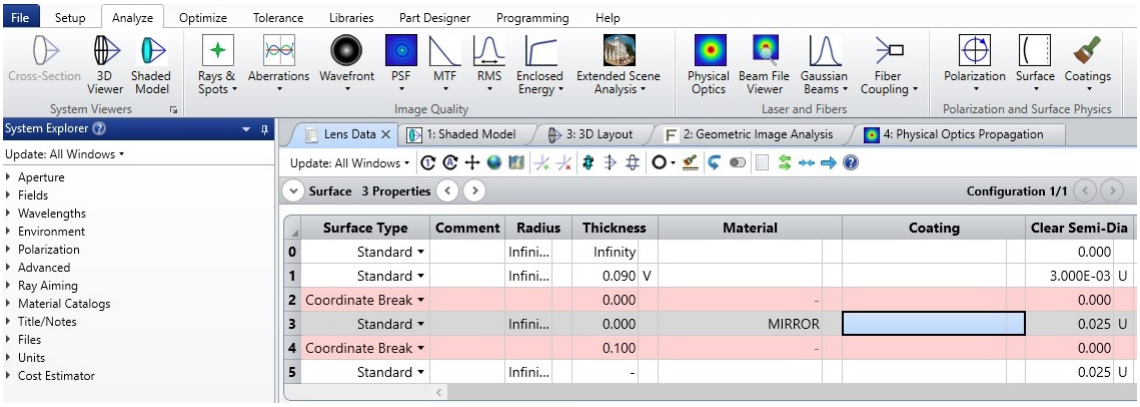

Fig. 3.7: Lens data setting in OpticStudio.

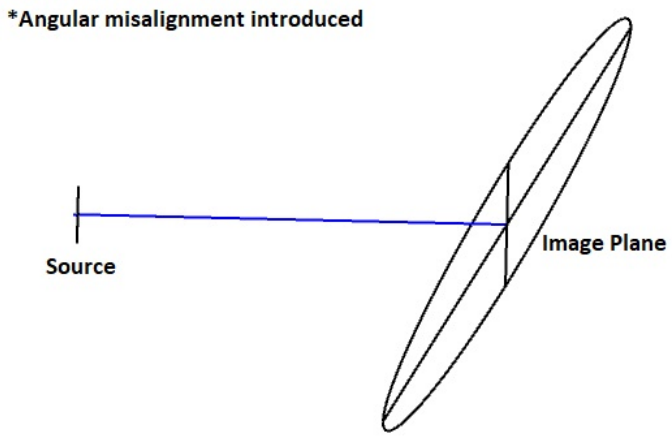

Fig. 3.8: Basic source-image plane misaligned setup.

3.6 Summary

In this chapter, two types of coupling calculation methods using CAD tool Zemax were discussed, the ray based approach and the wave based approach. The ray based approach is generally useful for fast simulation of systems which do not need detailed mode profile information. However, this method does not account for the optical beam waist and phase which greatly affect the coupling efficiency. The Physical Optics Propagation (POP) method uses a wavefront based approach that incorporates the phase information. This approach is more relevant to our coupling efficiency investigation. As such, the ray-based approach is only introduced here as a second method (non-sequential ray tracing) which finds its use for different applications such as illumination systems.

Chapter 4

Misalignment Effects in VCSEL-MMF Mode Coupling

4.1 Introduction

This chapter aims to explore the tolerance of an edge-coupled laser-fiber model and its effects on the coupling between the laser Low Order Modes (LOMs) and the fiber, as well as between the laser High Order Modes (HOMs) and the fiber. Misalignment between the laser and the fiber is rarely avoidable in the packaging of such systems such that studying its impact is crucial. But misalignment is not always unfavourable as measured or controlled decentralization can be useful in certain applications. Indeed, we can take advantage of this technique for different implementations. This chapter forms the basis for such an application in Mode Division Multiplexing(MDM) which is discussed in chapter 5.

4.2 Misalignment Effect in Parallel End-Coupled Model

Vertical cavity surface emitting lasers (VCSEL) coupled to multimode fiber links are key to a cost effective and practical solution for short reach high speed transmissions. Losses due to imperfect alignment of the structures are an important part of studying the VCSEL-MMF links. This can be understood as a basis to either avoid such losses or utilising them for a desirable application. Misalignment effects in laser- fiber structure is calculated via the ray tracing coupling efficiency approach in [47] which show similar trend to the results presented in this section with the wave based approach in section 4.4. Misalignment tolerance analysis based on theoretical model for Single Mode Fiber (SMF) is shown to increase coupling efficiency using a lens [48]. Parallel end-coupled structures offer ease in interconnecting optical ends without the use of micro or bulk-optical elements which complicate packaging process and are susceptible to decentralization leading to poor efficiency. Such mismatch in the alignments affect the overall coupling as well as the performance of the optical link. We report the effects of such misalignments on a mode-to-mode coupling basis for such VCSEL-MMF link to show the effect on Higher Order Modes (HOM) compared to Low Order Modes (LOM).

4.3 Modeling of the Coupling System

Figure 4.1 shows the Zemax shaded model (surfaces with different colouration) of the VCSEL-MMF parallel end-coupled setup with a separation of 50 μm. The Physical Optics Propagation (POP) and the analytical model use the same parameters for both the laser and the fiber. We set the parameters for a laser wavelength of 850 nm having the output beam waist of 3 μm. The multimode fiber type OM4 has a core and cladding diameter of 50 μm and 125 μm, and a refractive index of 1.45 and 1.435, respectively.

Zemax OpticStudio is used to simulate the VCSEL Laguerre-Gaussian (LG) free space modes coupled to the MMF Linearly Polarised (LP) modes extracted from the Lumerical MODE solutions as presented in chapter 3. This model is then compared with the analytical Coupling Efficiency (CE) of the LG modes and MMF LP modes [49],[50]. The analysis is done for a $\mathrm{LOM_{VCSEL}}$-$\mathrm{LOM_{MMF}}$ (LG00even-LP01) coupling and a $\mathrm{HOM_{VCSEL}}$-HOM $_{\mathrm{MMF}}$

(LG02even-LP21a). This comparison highlights the difference in the coupling effect of the LOM and the HOM.

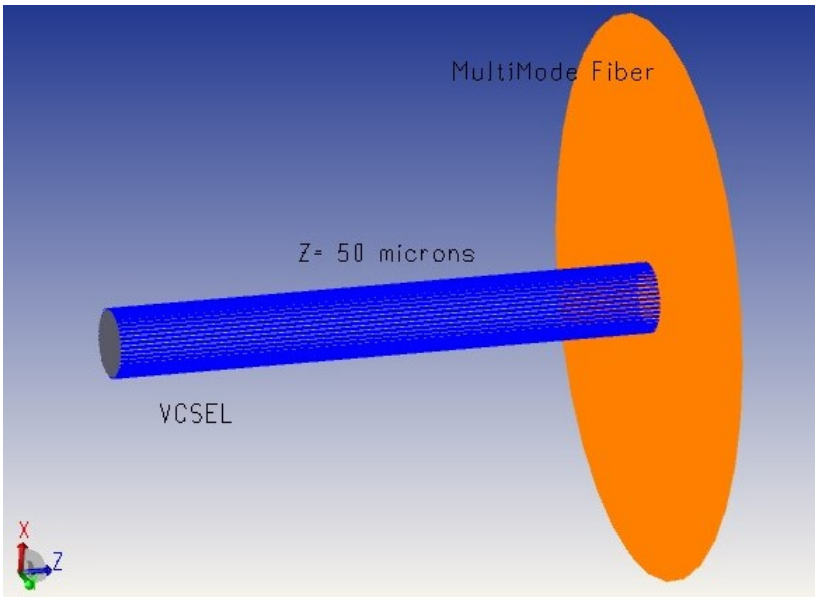

Fig. 4.1: Shaded model for the parallel end-coupled laser fiber link.

4.4 Observations and Discussion

This section highlights the effect of various misalignments observed in the parallel end-coupled model. The results are obtained for different lateral and radial displacements between the laser and the fiber. The data is tabulated and presented graphically to easily understand the trend and the difference in impact on lower order modes and the higher order mode coupling.

4.4.1 Variation with Distance

Table 4.1 below shows the variation in coupling efficiency with respect to the distance between the laser and fiber. As expected, it is observed that both the LOM and HOM coupling decreases with an increase in spacing.

Table 4.1: Variation in coupling efficiency as a function of the distance between VCSEL and fiber

Spacing (μm)	10	20	30	40	50
LG00e-LP01 (%)	68.04	67.12	65.66	63.86	61.59
LG02e-LP21a (%)	30.59	29.32	27.40	25.18	22.62
Spacing (μm)	60	70	80	90	100
LG00e-LP01 (%)	59.04	56.29	53.42	50.51	47.61
LG02e-LP21a (%)	19.94	17.29	14.80	12.52	10.49

Figure 4.2 illustrates the VCSEL-MMF coupling efficiency versus the spacing between the center of the VCSEL and the center of the MMF core. The 'A' and 'S' in the legend denote the analytical and the POP values obtained through simulation, respectively. From the table and figure it is observed that the effect of increasing free space distance is more adverse for HOM coupling than for LOM coupling. The coupling efficiency for the HOM coupling decreases by approximately 66% compared to 30% in the case of LOM coupling for the same separation of 100 μm. The loss can be attributed to the beam waist/divergence as well as the mode field diameter mismatch [51]. As such, packaging leading to variation in the laser-fiber spacing (distance) is responsible for coupling losses. Note that the spacing parameter is not the most detrimental factor in coupling losses. It is possible to avoid the coupling losses that arise due to spacing by having a fix separation mounts between the laser and the fiber which can be designed with precision for optical modules. This helps us to mitigate the ramifications of undesired spacing.

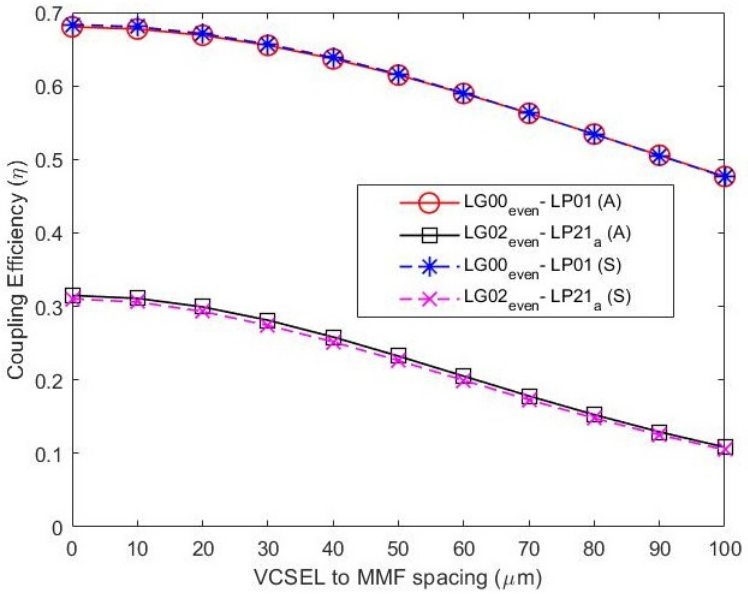

Fig. 4.2: VCSEL to MMF mode coupling efficiency variation with distance.

4.4.2 Impact of Offset Variations

Tables 4.2 and 4.3 show the variation in coupling efficiency with respect to the radial offset (X_{offset} and Y_{offset}) from the center between the laser and the fiber. The radial offset is an input in the lens data dock in OpticStudio. It is applied on the fiber modes which shifts the center of the mode by the defined units. The offset values are kept small to confine most of the mode optical power within the fiber core. Fig 4.3 shows a setup with 5 μm offset between the source and the fiber.

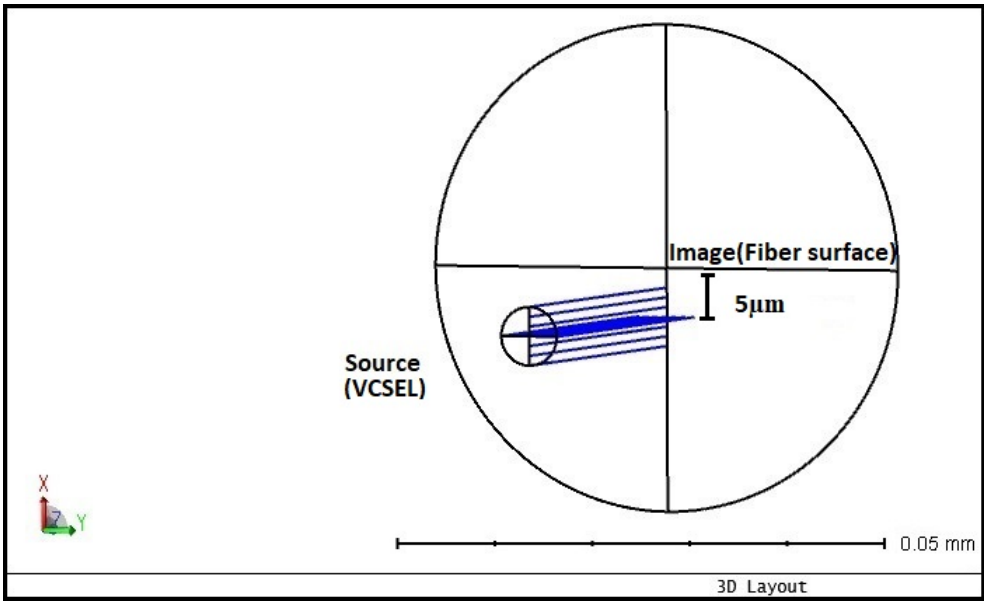

Fig. 4.3: Source-fiber(image) plane decentered setup.

Table 4.2: Variation in coupling efficiency as a function of X_{offset}

δX (μm)	-5	-3	-1	0	1	3	5
LG00e-LP01 (%)	19.49	40.17	58.31	61.59	59.60	42.90	21.74
LG02e-LP21a (%)	0.33	5.76	19.17	22.62	20.49	7.21	0.54

Table 4.3: Variation in coupling efficiency as a function of Y_{offset}

δY (μm)	-5	-3	-1	0	1	3	5
LG00e-LP01 (%)	19.46	40.15	58.31	61.59	59.60	42.88	21.71
LG02e-LP21a (%)	0.33	5.73	19.16	22.62	20.48	7.15	0.53

Figure 4.4 illustrates the coupling efficiency as a function of the decentralization of the fiber by a factor of δX/δY. The displacement in either X or Y direction has nearly the same values in both simulation and analytical results. The offset from the center of the fiber was calculated for up to an absolute maximum of 5 μm. This offset showed that the HOM coupling decreases by 98% as compared to 66% in the case of the LOM coupling. The spacing is fix to 50 μm.

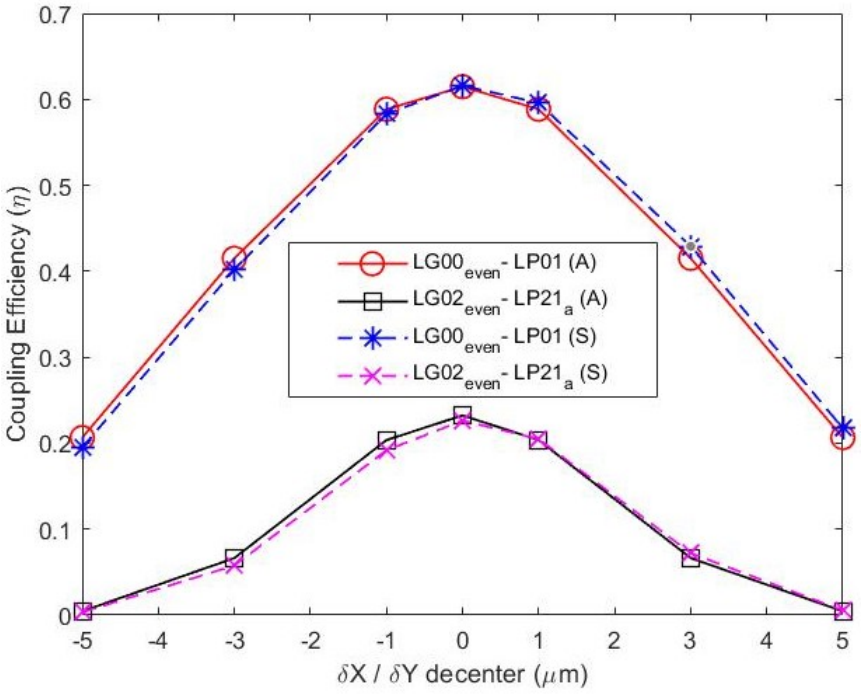

Fig. 4.4: VCSEL to MMF coupling efficiency variation with offset.

4.4.3 Coupling Variation with Tilt

Tables 4.4 and 4.5 below shows the variation of coupling efficiency with respect to the angular tilt (X_{tilt} and Y_{tilt}) between the laser and fiber. The tilt of the fiber mode is equivalent to adding a linear phase shift having an angled mode profile overlap. Fig 4.5 shows a setup with 5 ° tilt between the source and the fiber.

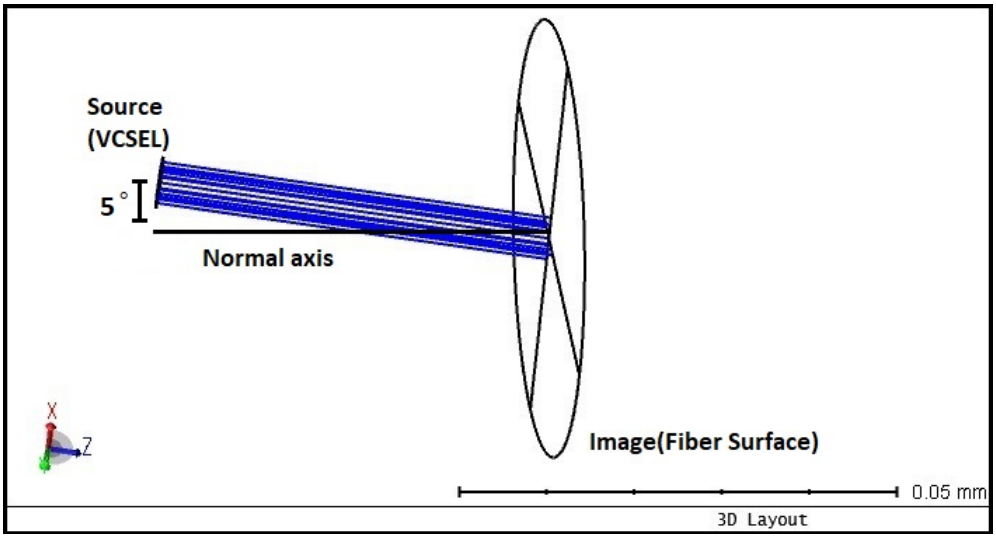

Fig. 4.5: Source-fiber(image) plane tilted setup.

Table 4.4: Variation in coupling efficiency as a function of X_{tilt}

$\delta\phi_x(^\circ)$	-5	-3	-1	0	1	3	5
LG00e-LP01 (%)	8.19	29.60	56.50	61.59	57.35	30.96	8.82
LG02e-LP21a (%)	1.23	2.59	17.43	22.62	18.23	2.83	1.09

Figure 4.6 highlights the effects of the angular misalignment (tilt) between the two mode coupling scenarios. The spacing between the laser and the fiber is kept the same (50 μm) to

Table 4.5: Variation in coupling efficiency as a function of Y_{tilt}

$\delta\phi_y(^\circ)$	-5	-3	-1	0	1	3	5
LG00e-LP01 (%)	8.82	30.95	57.35	61.59	56.50	29.60	8.19
LG02e-LP21a (%)	1.12	2.91	18.24	22.62	17.43	2.52	1.19

compare the result. The range of values for the tilt $\delta\phi_x/\delta\phi_y$ had similar results. The analysis was done for an absolute maximum tilt of 5°. The coupling for the HOM reduced by 95% as compared to a 86% decrease for the LOM. For more than 5° angled tilt the coupling value is close to zero.

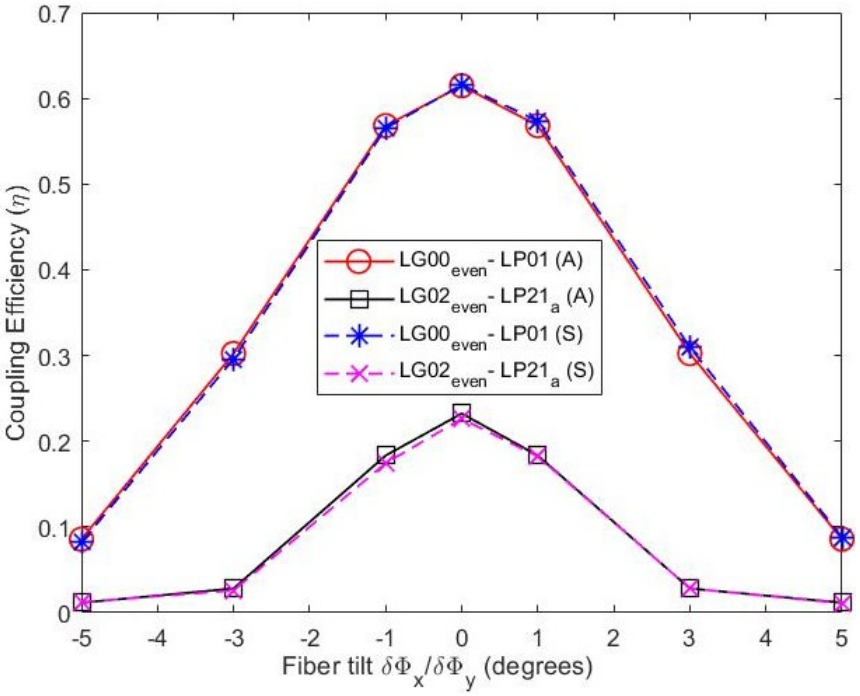

Fig. 4.6: Effect of tilt on coupling efficiency.

4.4.4 Discussion

From the results presented in the previous section, we observe that a small offset or small tilt between the laser and the fiber has a drastic effect on the coupling values. In fact, the coupling efficiency drops nearly to zero in the case of HOM coupling. The reason for such destructive effect can be attributed to the fact that the LOM are generally meridional rays traversing through the center of the fiber and are less affected by a small misalignment. Comparatively, HOM can be a combination of meridional rays and skew rays (rays not passing through the fiber axis) with most of the energy near the cladding. So any small misalignment in the longitudinal plane or the angular plane can make them more skewed thereby radiating out energy. This process in turn reduces mode matching and hence decreases the coupling efficiency. We can also verify the results of Zemax simulation for a combination of misalignments that may affect overall coupling which needs to be mitigated for effective transmission over the link. Tables 4.6 and 4.7 below show the variation of coupling efficiency with respect to the combined effect of radial offset and angular tilt between the laser and fiber at 50 μm spacing. We see that the values for the Zemax simulation are close to the values obtained analytically.

Table 4.6: Variation in coupling efficiency as a function of offset and tilt(Zemax)

Tilt (°), Offset (μm)	1,1	2,2	3,3
LG00e-LP01 (%)	55.50	39.12	21.55
LG02e-LP21a (%)	16.50	5.6	1.6

Table 4.7: Variation in coupling efficiency as a function of offset and tilt(MATLAB)

Tilt (°), Offset (μm)	1,1	2,2	3,3
LG00e-LP01 (%)	57.70	37.66	20.45
LG02e-LP21a (%)	16.00	4.86	0.95

4.5 Summary

We show the effects of misalignment in a edge-coupled laser fiber model using the POP in OpticStudio. The results are convincing in reference to the results obtained from the analytical method. This shows the importance of precision during the manufacturing and packaging of such setups. Deploying micro-optics along with the misalignment can be useful in different applications. The next chapter uses this method to discuss mode selective coupling links and benefits of misalignment on such systems.

Chapter 5

Mode Selective Coupling in VCSEL-Fiber Links

5.1 Introduction to VCSEL-MMF Links for High Capacity

As elaborated in chapter 2, MDM can be deployed to increase the capacity of the next generation of optical interconnects. In the literature, we also saw how selectively exciting the VCSEL modes enabled us to damp the effect of intermodal dispersion which can lead to better transmission through the fiber. In this chapter, we demonstrate a model depicting a laser to fiber coupling using basic micro-lens and misalignments to excite only the desired mode groups in the MMF using selective mode coupling. This presents a practical and cost-effective approach to obtain spatial division for MDM.

5.2 Zemax Model for VCSEL-MMF Micro-Optic Setup

Figures 5.1 and 5.2 show the Zemax model and the misaligned model of a VCSEL-MMF coupled setup through a plano-convex lens (N-BK7), respectively. Such lens type aids in reducing distortions due to spherical aberrations and is less expensive than its biconvex counterpart [52],[53]. The lens has a radius of 100 μm with a thickness of 5 μm and an aperture (opening of the lens) of 10 μm. The lens is inserted 10 μm after the VCSEL and 35 μm before the MMF. The Physical Optics Propagation (POP) and the modal overlap integral

use the same parameters (e.g., beam waist, fiber index profile) to compute the coupling. We simulate the results for a laser wavelength of 850 nm with an output beam waist of 3 μm. The multimode fiber has a core and cladding diameter of 50 μm and 125 μm, and a refractive index of 1.45 and 1.43, respectively.

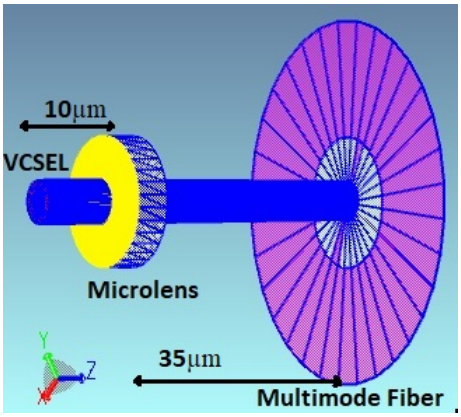

Fig. 5.1: Model of the setup in Zemax.

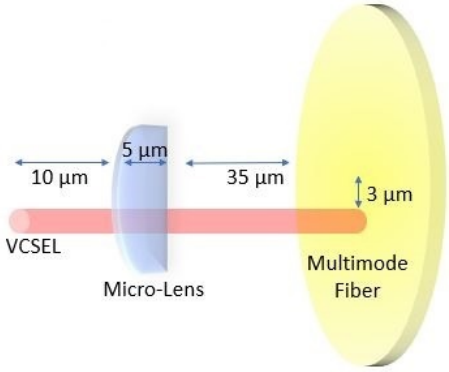

Fig. 5.2: Trajectory through micro-lens with an offset of 3 μm.

The POP features in Zemax provide the flexibility to simulate and select Laguerre-Gaussian (LG) modes (free space modes from a VCSEL) that are coupled to the MMF linearly polarized (LP) modes generated by the simulator MODE from Lumerical as seen in the previous chapters. We analytically validated this model methodology without the micro-optics in chapter 4. The coupling efficiency or power coupling efficiency (PCE) of LG modes and MMF LP modes is calculated using the overlap integral of the mode profiles for different variations in spacing, offset, and angular tilt [49],[50]. Figure 4.6 from chapter 4 highlights the normalized PCE to angular misalignment for two laser-fiber coupling scenarios where A and S denote the analytical and POP simulated values, respectively, and were a perfect match. Here, we further investigate two launching scenarios where in one, we excite the fundamental mode (LG00even) as it provides best PCE for the first mode group in the fiber, when compared to all other LGm0 modes (azimuthal index is zero for first fiber mode group) and also by the virtue of symmetry. Secondly, we excite a HOM (LG12even) which also provides optimum PCE for the third mode group for the same reason. Finally,

we compare the results of a center launching condition at an arbitrary 50 μm spacing to the selective-mode lensed coupling achieved with variations in the misalignment for a fixed spot size realized with the model shown in figure 5.2. As presented in [46], the lens in such system is useful in focusing the beam (desired modes) by magnifying it onto the fiber with a misalignment helping in reducing unwanted coupling into other modes. The focusing term in the LG equation is $\exp\left(-ik\frac{r^2}{2R(z)}\right)$ which is impacted by the lens as shown in the equation 3.1.

5.3 Results and Discussion

Figure 5.3 shows VCSEL-MMF normalized PCE using the LG00even mode as the input for the two launching conditions, the coupling through the lens utilizes a radial offset of 3 μm between the laser and the lens. This radial displacement gives an optimum condition for coupling into the first mode group of the fiber by reducing the coupling into the unwanted third and fifth mode groups by approximately 85% and 88%, respectively.

Figure 5.4 highlights the normalized PCE using the LG12even mode as the input. In this case, the coupling through the lens has an angular tilt of 1° between the laser and the lens. This angular misalignment also provides spatial variation from the center launch condition and good coupling into the third mode group of the fiber, suppressing the coupling into the fifth mode group by almost 75% of the coupled power as compared to the center launch.

The analysis is extended for a third coupling scenario where we use LG24even as the input mode to excite the fifth mode group only in the fiber. With the above model (Figure 5.2) without any misalignments, when we introduced a plano-concave lens with the same characteristics to keep the model consistent (radius of -0.1 mm) for a third coupling scenario we observe an improved coupling of 10.2% as compared to the center launch for the schematic shown in figure 5.5. Also, we see improved tolerance for radial misalignment of up to 2 μm and for an angular tilt up to 2° with 15% an 36% PCE loss, respectively, without other undesirable mode groups excited for the schematic shown in figure 5.6. The above results show that radial offset and angular tilt have more impact on the higher order mode group coupling as confirmed in chapter 4.

The proposed model utilizes decentralization for spatial division which makes it less

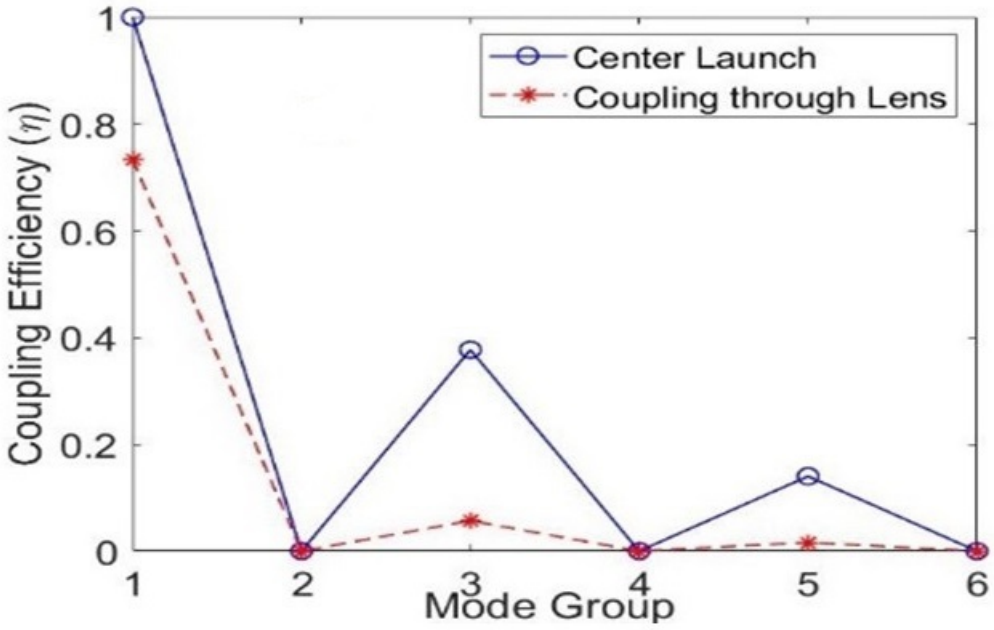

Fig. 5.3: Normalized PCE for different mode groups with LG00even input.

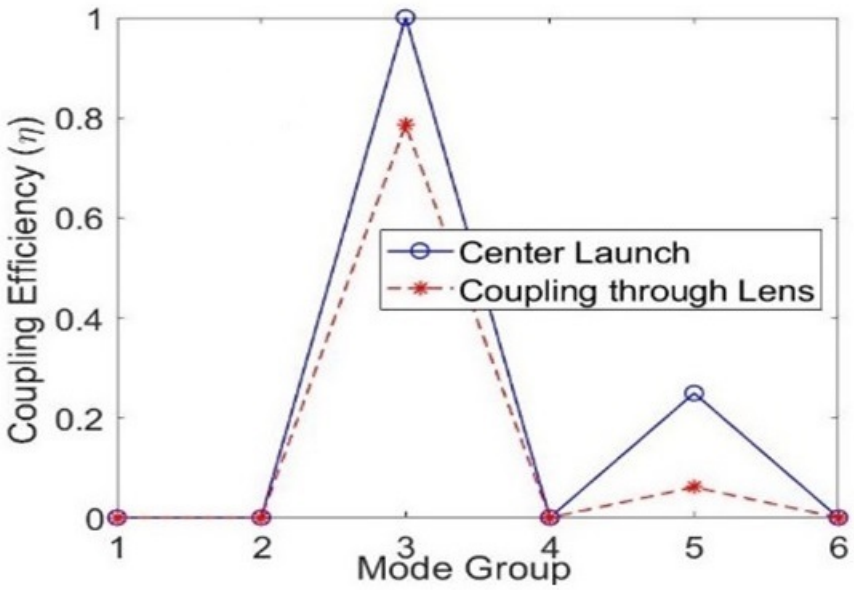

Fig. 5.4: Normalized PCE for different mode groups with LG12even input.

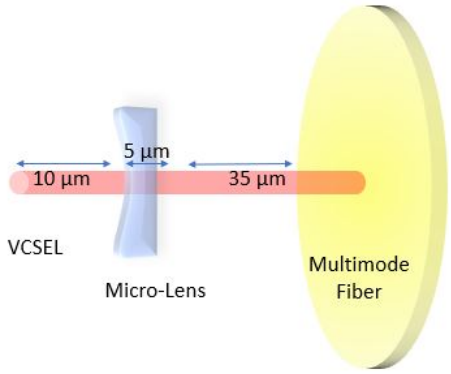

Fig. 5.5: Trajectory through a concave micro-lens with no offset.

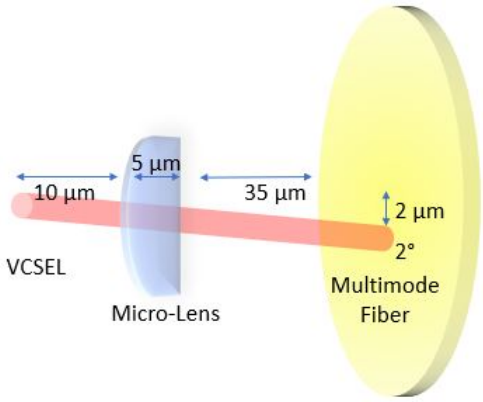

Fig. 5.6: Trajectory through the micro-lens with an offset and tilt of 3 μm and 3°.

susceptible to misalignments compared to a center launching scenario. This comes at the expense of lower PCE, while suppressing unwanted mode group excitation. This approach can potentially provide a practical solution in harnessing MDM in a transceiver module by reducing modal dispersion and mode partition noise in the fiber enabling spatial multiplexing by selecting the inputs based on the desirable mode groups in the fiber. The parametric values for the micro-lens and the setup can be varied to excite other mode groups with different input modes to extend the capability of the few mode VCSEL to MMF coupling. As in [54], this can offer solutions to optical MIMO to increase the data transmission capacity in such links.

5.4 Laser-FMF Links

Optimizing free space to FMF coupling with a theoretical approach indicates the importance of mode size matching [46]. The mode size or the mode field diameter can be the near field or the far field distribution of the mode, and is an essential parameter along with mode profile for efficient coupling. FMFs are also heavily used in different applications including fiber based lasers and sensors [55],[56],[57].

In this section, we use a two mode input namely LG00 even and LG02 even mode combined utilizing a Zemax macro program to create a Zemax multimode (ZMM) input having a beam waist of 3 μm for the setup shown in figure 5.7 to evaluate the selective mode input to FMF coupling. A Zemax macro program is a part of Zemax programming language which helps us to perform calculations based on user data. Zemax macro approach is different from the single mode inputs used in the previous chapters as it allows us to simulate multiple modes as input. The plano-convex lens used has a radius of 40 μm after we optimize its radius for increasing the coupling efficiency.

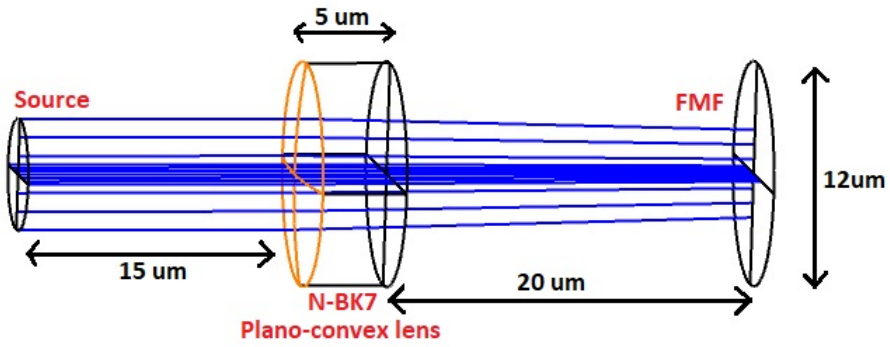

Fig. 5.7: Laser to FMF coupling setup in Zemax.

Figures 5.8 and 5.9 show the LG00 even and LG02 even mode, respectively.

First, the setup is coupled without the lens and for simplicity, the optical power allocated to both LG modes was equal at source. This kind of selective inputs are important for multiplexing application using FMF. These selective modes or combination of modes can be created or manipulated by using diffraction elements or dielectric metasurfaces to change the direction of light creating low order LG or high order LG modes [37],[38]. The reason

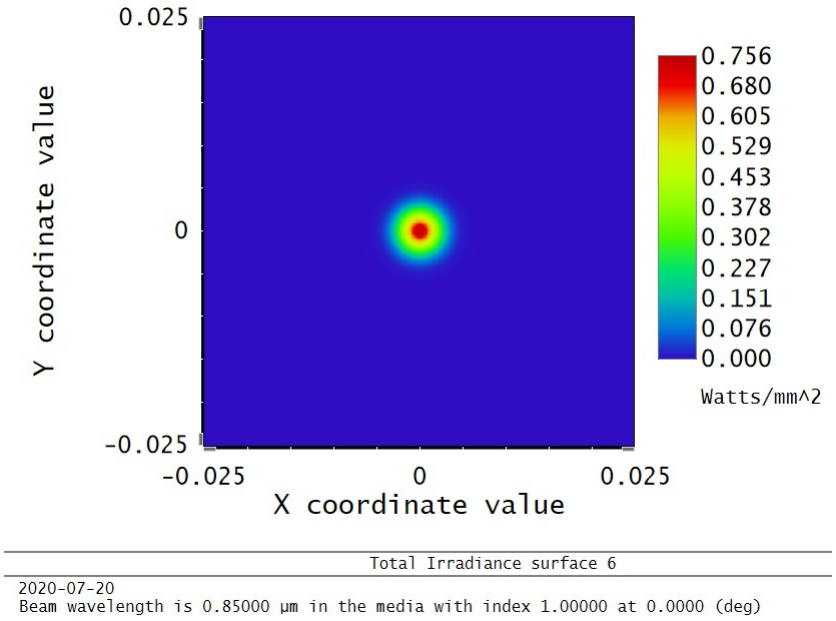

Fig. 5.8: LG00 even mode for creating Zemax multimode with the x-axis and y-axis representing the distance in nanometer.

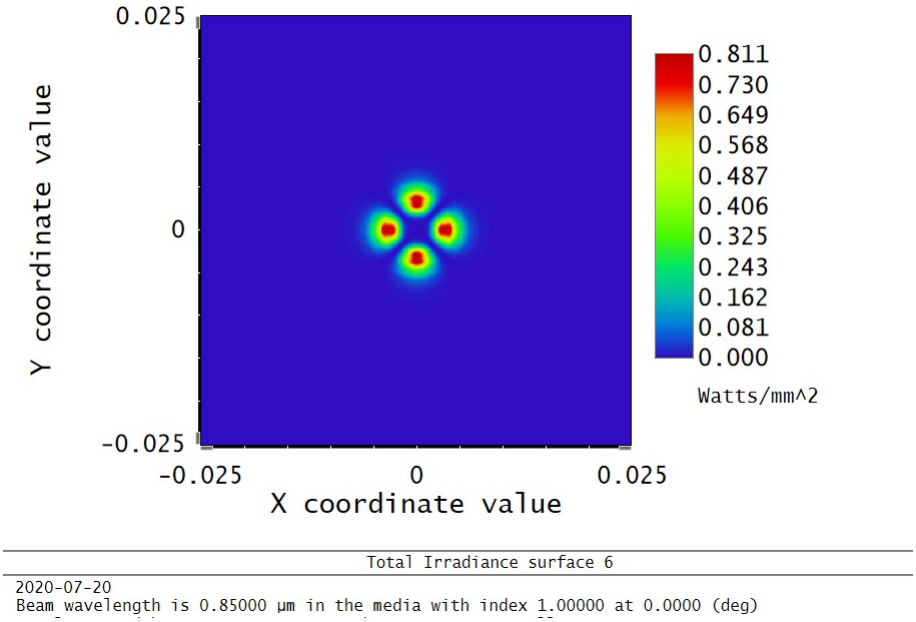

Fig. 5.9: LG02 even mode for creating Zemax multimode with the x-axis and y-axis representing the distance in nanometer.

behind selecting the two modes is because they mostly support two different mode groups in the fiber, namely the first and the third respectively. Figure 5.10 shows the combined LG00 even and LG02 even mode at the fiber surface. The total coupling value for all the supported mode groups (first five mode groups) in the GI fiber (core 6 μm) is observed to be around 63% with mode group one and three sharing approximately 30.5% and 24% power respectively with other mode groups sharing low or no power. As the combination of two modes (ZMM) predominantly excite two different mode groups in the FMF, it mitigates Inter Symbol Interference (ISI) or modal dispersion thereby enabling high capacity data links [33].

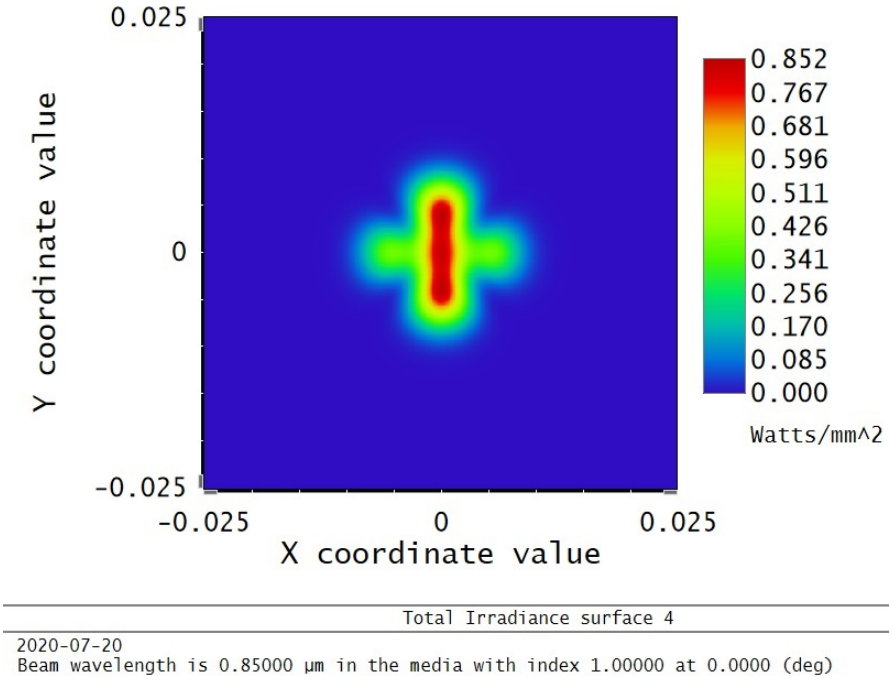

Fig. 5.10: Combined ZMM observed at the fiber surface with the x-axis and y-axis representing the distance in nanometer.

The performance of such a system can be increased using the micro-optics as shown below in figure 5.11. The total coupling value for all supported mode groups increased to approximately 92% with mode groups 1 and 3 sharing 47% and 43% power, respectively, which was around 97.8% of the total power coupled as compared to the 63% without the

micro-optics. The imaging lens magnifies the mode for a better match than the lens-less case. This allows fair distribution of optical power between the two mode groups and can be used as two different data channels to double the data capacity while lowering the inter-channel interference. As shown in [37] for a VCSEL-MMF setup, similarly here each mode from different VCSELs can be modulated separately with different data stream before combining for a VCSEL-FMF setup. This allows higher volume per channel as compared to the conventional link where each channel is modulated at a single desired frequency.

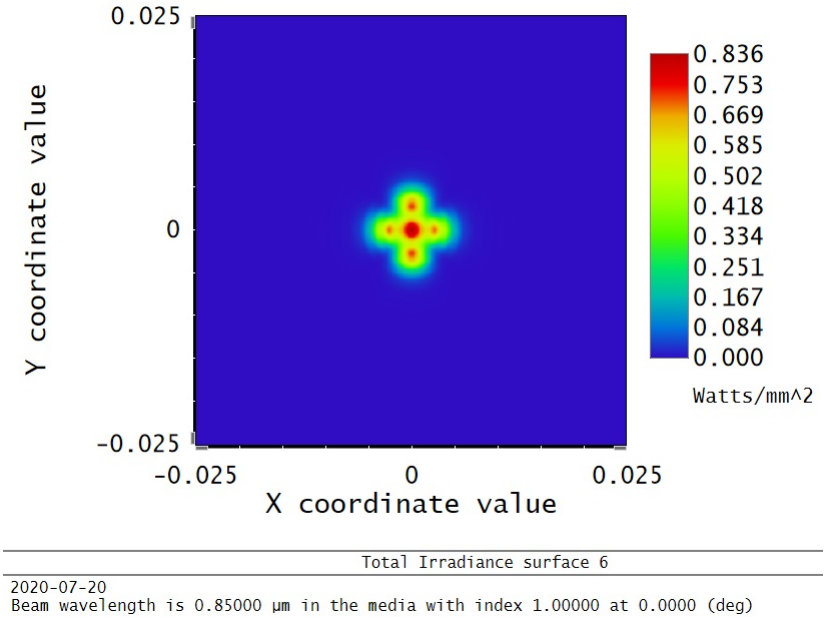

Fig. 5.11: Combined ZMM observed at the fiber surface improved with lens with the x-axis and y-axis representing the distance in nanometer.

5.5 Summary

In this chapter, we discussed the advantage of micro-optics in the laser-fiber misaligned setup for the application of Mode Division Multiplexing (MDM). The magnification of the modes for better coupling was achieved using a thin lens. We demonstrated three different launching conditions to excite three different mode groups in the fiber while attenuating the

others. Each of these channels can be used to transmit data independently to increase the overall bandwidth of the system. A brief discussion on Laser-FMF links for MDM application was also presented. We demonstrated a 2 input MDM on an FMF link utilising the micro-optics and misalignment to improve the total coupling efficiency from 63% to 98%. This allows to have more data on different channels on the same fiber lane. This also enables not implementing complex modulation formats that may increase ISI during reception and decoding.

Chapter 6

Coupling Efficiency Analysis of 45° Angled MMF Facet

As mentioned in chapter 1, I did the simulation work on the design and helped in brainstorming the fabrication ideas. The fabrication is from SiJ Technologies, and the setup measurements were performed by my colleague Dr. Reza Nezami, a postdoctoral student in our research team at McGill, along with Dr. David Rolston and other fellow colleagues at Reflex Photonics (now Smiths Interconnect) at their facility in Kirkland, Canada.

6.1 Introduction

One of the most popular structures currently utilized in the optical transceiver modules deploy a design which includes a laser, vertically emitting light which is then reflected by a 45° polished fiber to guide the light into the core with having similar structures at the receiving end of the fiber for coupling into the photodiode as well. This design has an advantage of requiring less complex packaging compared to a back-to-back coupled design. Such an arrangement generally align multiple arrays of laser to the fiber facet for having multiple channels for transmission or reception. Figure 6.1 shows such a layout at the transmitter side of the setup.

The laser is facing the angled fiber which is having a 45° reflecting surface preferably with gold coating making the optical power reflect inside after striking the gold surface.

The coupling efficiency of such a structure is determined by how well the free space modes transfer their energy to the fiber modes which is a product of both the ratio of optical power emitted by the laser to the optical power received at the fiber and the ratio of optical power received by the fiber to the optical power coupled into the modes of the fiber.

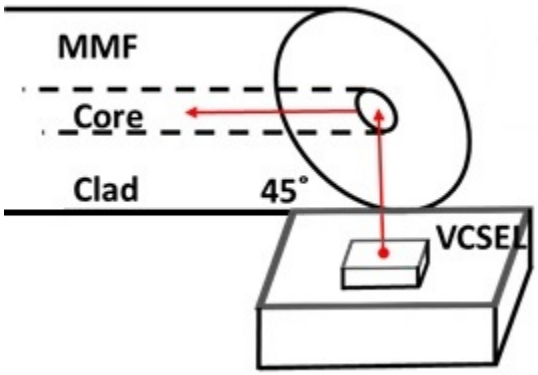

Fig. 6.1: Conventional 45° reflecting type fiber surface at transmitting side.

6.2 Simulation Methodology

Zemax was used to first calculate the coupling of the free space fundamental LG mode to a first few modes of the fiber such as LP01, LP02, etc. We then recalculate the coupling of the same modes after modifying the 45 degree reflecting surface to a concave (curved inward) reflecting surface. A concave structure is useful in converging more light on the desired axis similar to a convex lens. As the beams from laser sources tend to have a divergence angle, this structure helps in capturing more light than a plane reflecting surface. This customization enabled us to focus in more light thereby increasing the possibility of having a better mode field profile match as compared to the conventional structure. It is demonstrated that the Mode Power Distribution (MPD) is not uniform and the low order modes carry most of the power without misalignments [17]. This approach was also used for other input-output mode combinations (example, LG02 even as input). After this simulation, the curved lens structure was fabricated to mimic the simulation design, modifying it to a micro mirror after

gold deposition technique. The fabrication process is described in the following sections.

6.3 Simulation Results: Conventional vs Modified structure

6.3.1 Model and Coupling

Figure 6.1 above shows the conventional structure and figure 6.2 below shows the reference curved mirror structure in free space. The curved image is extracted out of Zemax's shaded model design. The source (laser) to the mirror distance is kept at 50 μm. The image plane is at a distance of 25 μm from the mirror having a radius of -0.3 mm. All the other Physical Optics Propagation (POP) settings are kept the same throughout as in the previous chapters. The coupling measurement for the conventional structure (plane mirror) and the

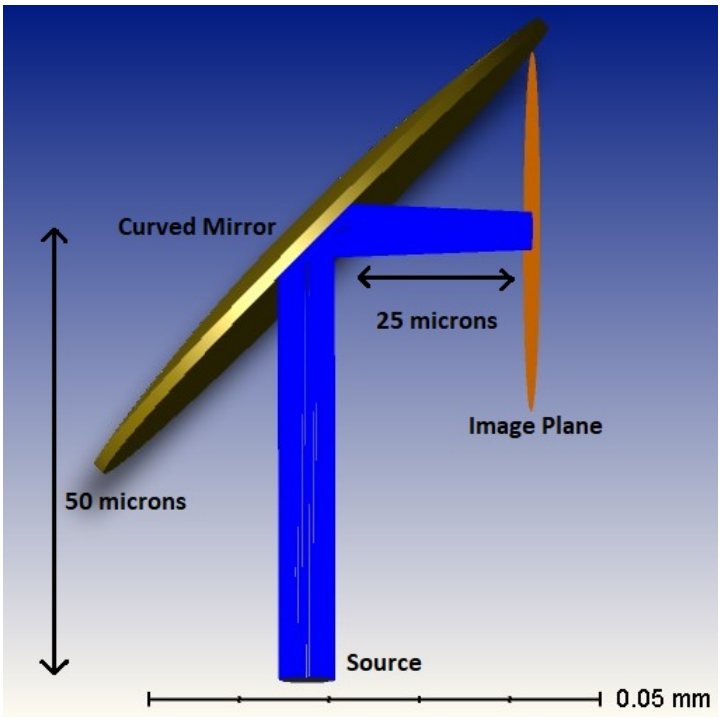

Fig. 6.2: Modified concave reflective structure.

curved structure are shown below for the fundamental LG (Laguerre-Gaussian) input beam having a beam waist of 3 μm to the fundamental mode and a few other modes of the

fiber having similar electric field profiles (for dissimilar profiles, *i.e.*, having a different field profile than the input mode, the efficiency was close to nil). For example, the coupling efficiency for LG00e-LP23a was observed to be close to 0. Table 6.1 below records the coupling coefficients observed in the Physical Optics Propagation tab in OpticStudio. The coupling values are taken just outside the reflecting surface to mimic the actual fiber core setup coupling. The concave surface (different radii) had a better overall coupling efficiency for the setup compared to the plane reflecting surface. The table 6.1 shows the observed coupling as a function of the radius. The primary reason for the better coupling being better mode profile overlap which was inhibited in case of the plane reflector due to laser beam divergence. This initial simulation formed the basis of the fabrication of such curved structures which are discussed in the following sections.

Table 6.1: Variation in coupling efficiency as a function of the radius of the mirror

Radius of mirror(mm)	LG00e-LP01	LG00e-LP02	LG00e-LP03	Total coupling(%)
Infinite	29.14	18.88	11.80	59.82
-0.2	59.07	11.53	20.1	72.61
-0.3	48.30	18.86	6.12	73.28
-0.4	42.73	20.37	8.66	71.76

6.3.2 Effect of Misalignment and Reflective Coating

We observed improved coupling in the modified structure as shown in table 6.1. There are different parameters which can affect the above coupling. Misalignment between the laser-mirror and the poor reflective coating of the mirror being of utmost importance. As discussed in chapter 4, the angular misalignment have adverse effect on the coupling. Table 6.2 shows the effect of 1° misalignment between the laser-mirror. This minute difference results in the efficiency to drop by more than 40% which is even poorer than the conventional structure. This can be considered as a potential drawback of this modified structure as it is more sensitive to misalignments.

The reflective coating of the mirror is another aspect which is important when fabricating the design. There can be different materials that can be simulated in Zemax. In this work,

Table 6.2: Variation in coupling efficiency with a 1° misalignment between laser-mirror

Radius of mirror(mm)	LG00e-LP01	LG00e-LP02	LG00e-LP03	Total coupling(%)
-0.3	32.71	7.89	3.07	43.76

we discuss silver and glass. Silver ink is a cost effective alternative which has its reflecting efficiency close to gold at 850 nm but can be prone to corrosion in longer run. Reference [58] compares the reflectivity of gold and silver inks. We discuss glass to highlight the fabrication results presented later, which were observed due to poor coating of gold on the epoxy. Table 6.3 shows the coupling efficiency variation with the choice of reflecting material for the mirror. It is observed that a poorly coated epoxy will have detrimental effects on the coupling efficiency of the modified structure as most of the light can pass or scatter through the structure without being reflected into the fiber. Also, it is noted that the combination of the misalignment and coating effects can simultaneously reduce the coupling efficiency of the setup.

Table 6.3: Variation in coupling efficiency with different reflecting material

Radius of mirror (mm)	Material	Total coupling (%)
-0.3	Gold	73.28
-0.3	Silver	72.71
-0.3	Glass	2.07

6.4 Fabrication Process and Technique

There are various techniques which can be used to fabricate the micro-optics or specifically the microlens structures over the fiber tips with varying resolution and precision. Most commonly used techniques include epoxy stamping, inkjet printing or drop on demand methods. Figure 6.3 shows the basic setup of the inkjet drop on demand method. The piezo-electric or the heat element in the printer is fed by the data along with a control signal which can affect the size or the duration of the drop. The ink used will have a specific viscosity range as per requirement as described in subsection 6.5.1. The ink used can also be conductive, such as

the UltraViolet (UV) ink, etc. The choice of ink depends on the type of curing technique to be deployed. The nozzle helps the ink to drop on the substrate forming the desired shape and size of the lens.

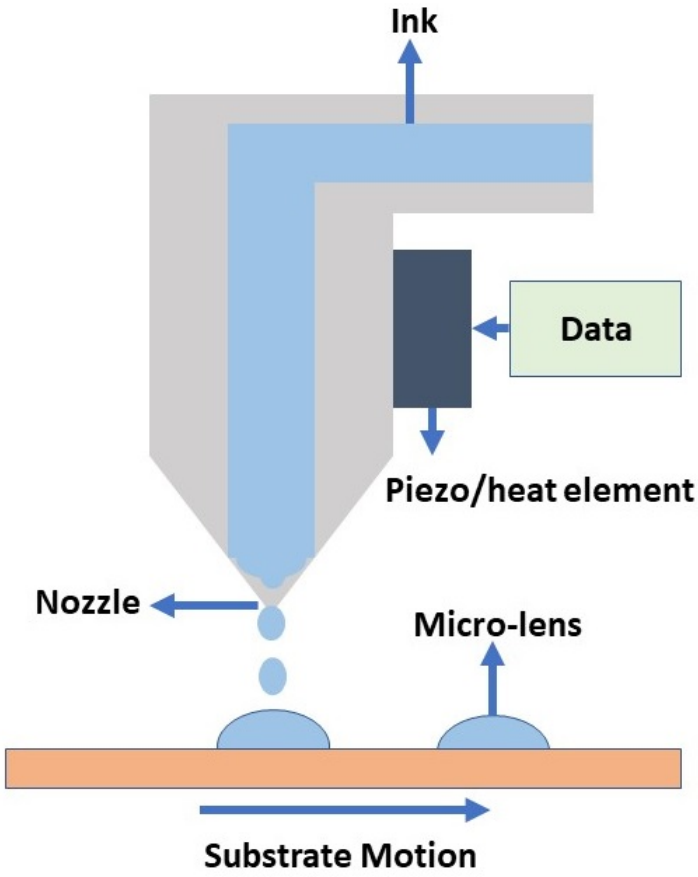

Fig. 6.3: Basic setup defining the process of inkjet printing of micro-lens.

The lens fabrication requires the process to be definite at a really small scale or at the micron level. There have been advances in the technologies which enabled a wide range of different lenslets to be fabricated having diameters from 20 μm to 5 mm at a large scale with high efficiency [59][60].

One of the prospective products that can enable us to define and characterize the micro-

lens is a Super Inkjet Printer [61]. This allows us to limit the volume of the drop to a very small value which improves the precision. The ability to maneuver a large variety of fluid inks with varying viscosity also makes it appreciable.

6.5 Initial Fabrication Outcomes

6.5.1 Type of Epoxy

Epoxy resin material plays a significant role in the development of the micro-optic structures. There are various concerns when choosing a resin which include but are not limited to the index of refraction at the concerned wavelength, available curing techniques for that material and the limit of transparency at a range of working wavelengths. One of the materials which we used as the epoxy is EPO-TEK 353ND from Epoxy Technologies [62]. The material is having a viscosity range of 3000 cPs-5000 cPs at room temperature and is ideal for alignment of optics including the V-groove ferrules at the working wavelength of 800 nm - 1000 nm with the transmission coefficient of more than 98%. The resin has a fairly high shelf life with a curing temperature of around 150° C.

6.5.2 Modified Structure

Figure 6.4 shows the modified fiber groove structure. The process includes two main steps. First, epoxy is deposited on the the fiber grooves manually for the initial sample therefore, the thickness, shape or the curvature of the epoxy hence deposited cannot be controlled by this technique. For better accuracy the techniques shared in section 6.4 should be followed. The epoxy is then cured at 150° C as discussed in section 6.5.1. The second step is gold deposition on the cured epoxy. This step is the foundation of such a structure because it gives the reflecting surface to the mirror. There are various process such as sputtering which may be used for this step [63].

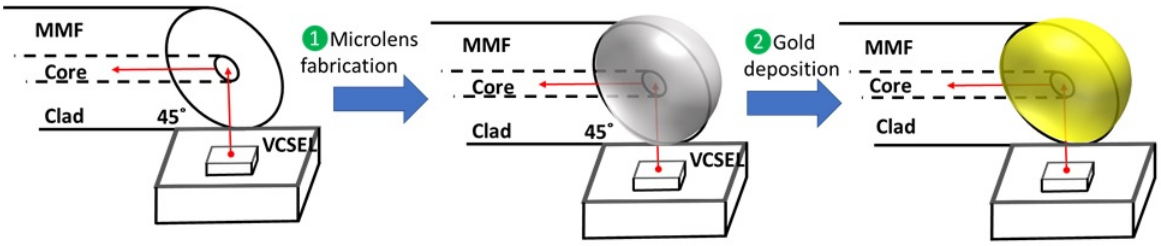

Fig. 6.4: Modifying the conventional reflective structure.

6.5.3 Test Setup

Initial Setup

Figure 6.5 shows the setup for initial fabrication procedure. The epoxy is manually dropped on the optical ferrules in the alignment setup forming a convex shaped lens at the tip of the fiber. The next step is to cure the epoxy so that it is ready for the gold deposition process. This converts the convex lens on the tip of the fiber into a concave reflecting mirrored surface. The drawback in this approach is the controlling of the radius or the thickness of the epoxy which can change the amount of coupling as discussed in section 6.3.

Gold Depostion

Figure 6.6 shows the optical ferrules after the gold deposition. In the figure, if we compare the deposition on the curved mirror compared to the flat mirror we see that the gold does not hold strong adhesive on the cured epoxy structure (dark regions visible). So, the coating on the modified structure is not good when compared to the conventional ferrule structure. The gold does not hold well onto the epoxy possibly due to weak bonding between the epoxy and the gold particle layer.

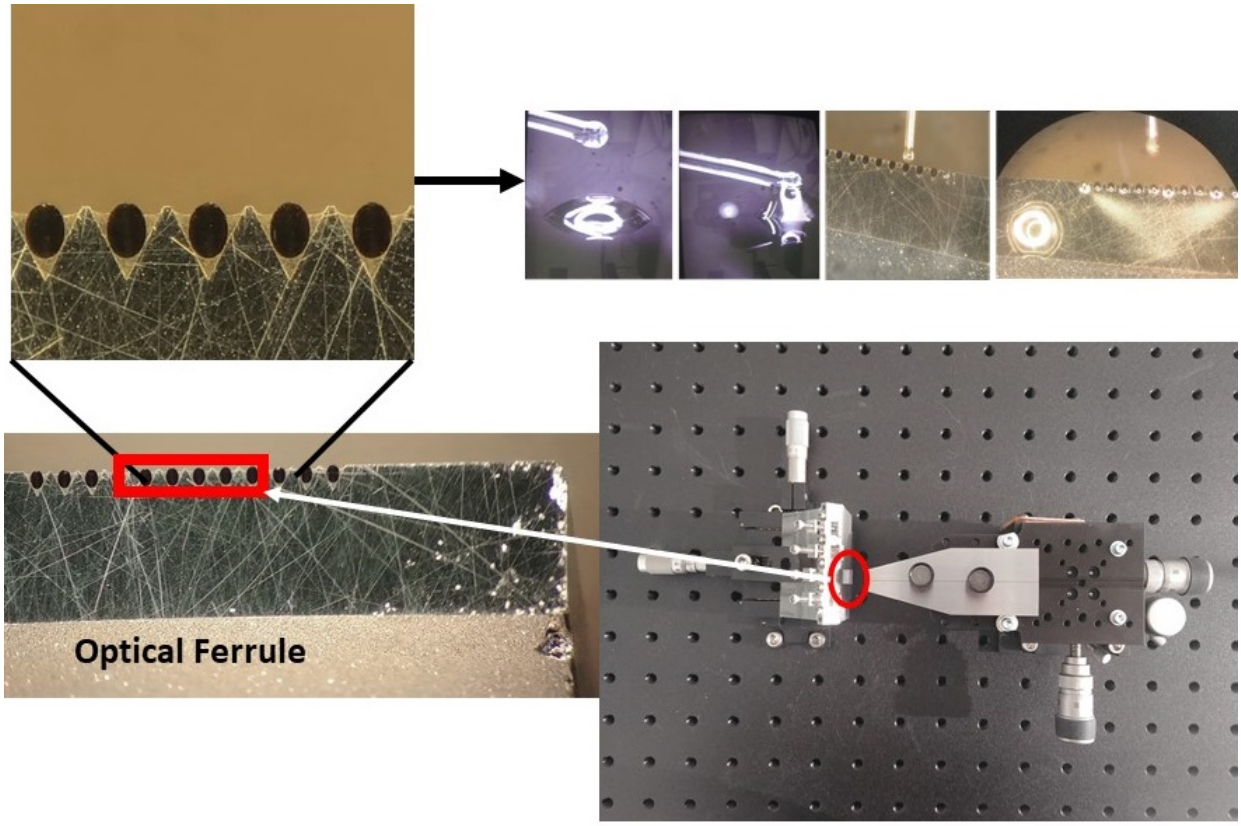

Fig. 6.5: Initial fabrication process before the curing and gold deposition ©Smiths Interconnect.

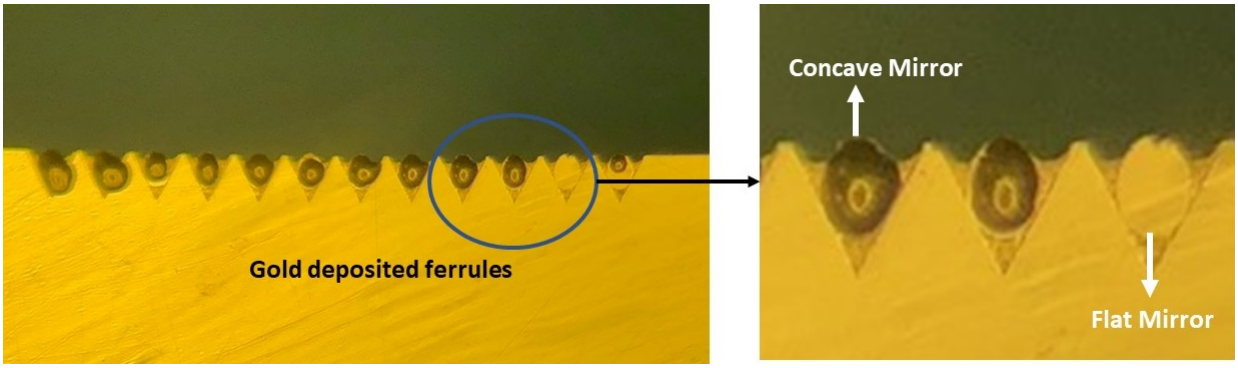

Fig. 6.6: Gold deposition on the optical ferrules after curing (flat and concave) ©Smiths Interconnect.

6.5.4 Results

After the preparation of the initial manually modified samples, the performance (reflectance and power coupled) is tested against the conventional samples.

The reflectivity from the flat mirror samples stood as high as 88% whereas the the same of the concave mirror stood at somewhere between 8%-48%. This is considerably poor as good adhesive coating is important for better reflectivity. The average power coupled per channel (fiber) for the conventional structure is observed to be around 2.10 mW. The power per channel for the modified structure was observed to be close to 0 mW. There were many possibilities which surrounded this observation. The measurement setup (ferrule to sensor distance) may not be optimum for the concave structure as the precision lies in the mm range. As the radius could not be controlled by manual deposition, the focal length may be short/long which makes the beam not converge at the sensor. It is also possible that not having the correct alignment when the VCSEL beam enters the ferrule affect the coupling. This is observed when the VCSEL array is aligned in a trial with utilising a "shim" (a thin strip of material to align parts) to produce about a 1° tilt. The coupled power observed in this case went upto about 2.01 mW from 0 mW which was a huge improvement and was comparable to the flat mirror ferrule power. This can be due to the fact that the misalignment helped in reflecting some power from the poorly coated structure in figure 6.6.

This provided more room for improvement in both the fabrication part and the setup. More tests and comparisons are further needed to establish better outcomes in the experimental setting.

6.6 Summary

This chapter demonstrates the analysis of coupling efficiency for the modified 45° angled fiber groove setup generally deployed in the high capacity short reach transmitters. The simulation results in Zemax provided an initial insight for the inception, fabrication and testing of such structures. Values close to the conventionally used fiber grooves were achieved in preliminary experiments and further study and analysis are required for better values in the application of the concept.

Chapter 7

Summary and Future Work

7.1 Summary

We highlighted the advantages of photonics and discussed the need for high capacity data networks. We also explained the theory of VCSELs and MMF along with the developments in the field over the years. Introduction to two different types of coupling methods, the GIA based approach and the POP based approach in Zemax was presented. The POP or the wavefront based approach incorporates the phase information for modes. This coupling method was used for the subsequent chapters. In the following part, we discussed the effects of misalignment in a parallel end-coupled laser fiber model. The results obtained through simulations were inline with the analytical values. This highlighted the importance of precision during the manufacture and packaging of such setups. Utilizing micro-optics along with misalignment formed the basis to discuss Mode/Space Division Multiplexing in the next part where the focusing/magnification of the modes for better coupling was achieved using a thin lens.

The misalignment trends presented in [47] showed similar direction to the results we obtained using the sequential model. The results were further improved using micro-optics. Table 7.1 below shows only the different parameters which were used to improve the coupling results in the misalignment trends presented in chapter 4.

A short analysis on Laser-FMF links for MDM application was also discussed as having potential to improve data rate on channels. Finally, the last chapter targeted on improving

Table 7.1: Table highlighting improvement in misaligned coupling with parameters

Mode group	Lens parameter used	Misalignment	PCE improvement
MG 1	Radius (focal power)	Offset (decenter)	From 20% to 75%
MG 3	Radius (focal power)	Tilt (angular)	From 50% to 80%

the coupling efficiency for the modified 45° angled fiber groove setup generally deployed in the high capacity short reach transmitters. Micro-mirror structures were simulated in Zemax provided an initial calculations which was followed by fabrication and testing of the modified structures. The results close to the conventionally used fiber grooves were observed in early trials. Additional study and analysis is still essential for better inception of the idea.

7.2 Future Scope

The future work in this section can be extended upon the current progress of the results based on chapters 5 and 6.

- Chapter 5 discusses the application of end-coupled links with the help of thin micro-optics for SDM applications. The next step in this setup is to characterize the total system performance after the transmission through the fiber. It is required to model the fiber propagation to receive the output eye diagrams to analyze the effect of intermodal noise, dispersion, absorption and other macro-micro losses. Zemax does not allow the propagation of modes through the fiber effectively as the fiber has to be created as a non sequential component which used ray tracing for traversal. Replacing MMF by FMF provides the elimination of fair share of higher order modes which affect the noise. Transmission of signals over such FMF links may provide additional channel for higher capacity with less impairments. Lensed tip fibers can also be fabricated which conform to the requirements if necessary as the FMF design utlised same focus lens for the combined input application.

- Chapter 6 discusses the fabrication of concave reflecting surfaces for commercially used V-grooved fiber coupling setups. As highlighted in the results, there is an eminent need to design the curved surface based on the specification of the actual VCSEL used in the

setup, for example the beam waist, the free space coupling distance, and the divergence of the beam available through data sheet and experiments. There is also potential in upgrading the material of the epoxy and the radius of the mirror so that after reflection the beam has a better far focus inside the fiber. Radius that is too short or too long can create near focus, aberrant convergence or infinite and divergent beams. This model is based on single converging surface as it was easy to fabricate for initial testing. The alignment is very sensitive and it is paramount to study the above parameters for optimum setting and effective coupling.

References

[1] Cisco, "Cisco Visual Networking Index: Forecast and Trends, 2017-2022 White Paper," https://www.cisco.com, (Last accessed: October 15, 2020).

[2] A. Thorley, "Moore's Law and Optical Fibre Bandwidth," https://blog.ecitele.com/moores-law-and-optical-fibre-bandwidth, (Last accessed: October 15, 2020).

[3] R. Essiambre and R. W. Tkach, "Capacity Trends and Limits of Optical Communication Networks," *Proceedings of the IEEE*, vol. 100, no. 5, pp. 1035–1055, 2012.

[4] O. America, *Fiber Optics Handbook: Fiber, Devices, and Systems for Optical Communications*, ser. McGraw-Hill field manuals. McGraw-Hill Education, 2001. [Online]. Available: https://books.google.ca/books?id=VJqsWHR9asoC

[5] J. Pozo and E. Beletkaia, "VCSEL Technology in the Data Communication Industry: The advantages, challenges and new opportunities that single-mode VCSELs bring in datacom," *PhotonicsViews*, vol. 16, no. 6, pp. 21–23, 2019.

[6] R. Michalzik and K. J. Ebeling, *Operating Principles of VCSELs*. Berlin, Heidelberg: Springer Berlin Heidelberg, 2003, pp. 53–98. [Online]. Available: https://doi.org/10.1007/978-3-662-05263-1_3

[7] T. Lee, "Recent advances in long-wavelength semiconductor lasers for optical fiber communication," *Proceedings of the IEEE*, vol. 79, no. 3, pp. 253–276, 1991.

[8] Z. Yin and X. Tang, "A review of energy bandgap engineering in III–V semiconductor alloys for mid-infrared laser applications," *Solid-State Electronics*, vol. 51, no. 1, pp. 6 – 15, 2007. [Online]. Available: http://www.sciencedirect.com/science/article/pii/S0038110106004035

[9] C. A. Rothenbach and M. C. Gupta, "High resolution, low cost laser lithography using a Blu-ray optical head assembly," *Optics and Lasers in Engineering*, vol. 50, no. 6, pp.

900 – 904, 2012. [Online]. Available: http://www.sciencedirect.com/science/article/pii/S0143816611003617

[10] J. J. Wierer Jr., J. Y. Tsao, and D. S. Sizov, "Comparison between blue lasers and light-emitting diodes for future solid-state lighting," *Laser & Photonics Reviews*, vol. 7, no. 6, pp. 963–993, 2013. [Online]. Available: https://onlinelibrary.wiley.com/doi/abs/10.1002/lpor.201300048

[11] Y. Zhang, H. Dong, R. Wang, J. Duan, A. Shi, Q. Fang, and Y. Liu, "Demonstration of a home projector based on RGB semiconductor lasers," *Appl. Opt.*, vol. 51, no. 16, pp. 3584–3589, Jun 2012. [Online]. Available: http://ao.osa.org/abstract.cfm?URI=ao-51-16-3584

[12] P. Moser, J. A. Lott, G. Larisch, and D. Bimberg, "Impact of the Oxide-Aperture Diameter on the Energy Efficiency, Bandwidth, and Temperature Stability of 980-nm VCSELs," *Journal of Lightwave Technology*, vol. 33, no. 4, pp. 825–831, 2015.

[13] B. W. Tilma, M. Mangold, C. A. Zaugg, S. M. Link, D. Waldburger, A. Klenner, A. S. Mayer, E. Gini, M. Golling, and U. Keller, "Recent advances in ultrafast semiconductor disk lasers," *Light: Science & Applications*, vol. 4, no. 7, pp. e310–e310, 2015.

[14] N. I. Zanoon, "The phenomenon of total internal reflection and acceleration of light in fiber optics," *International Journal of Computer Applications*, vol. 975, p. 8887, 2014.

[15] C. Pollock and M. Lipson, *Integrated Photonics*. Springer US, 2003. [Online]. Available: https://books.google.ca/books?id=7zvsOyljCMcC

[16] D. Marcuse, "The impulse response of an optical fiber with parabolic index profile," *The Bell System Technical Journal*, vol. 52, no. 7, pp. 1169–1174, 1973.

[17] T. H. Wood, "Actual modal power distributions in multimode optical fibers and their effect on modal noise," *Opt. Lett.*, vol. 9, no. 3, pp. 102–104, Mar 1984. [Online]. Available: http://ol.osa.org/abstract.cfm?URI=ol-9-3-102

[18] A. Yariv and P. Yeh, *Photonics: Optical Electronics in Modern Communications*, ser. Oxford series in electrical and computer engineering. Oxford University Press, 2007. [Online]. Available: https://books.google.co.in/books?id=B2xwQgAACAAJ

[19] B. Saleh and M. Teich, *Fundamentals of Photonics*, ser. Wiley Series in Pure and Applied Optics. Wiley, 2007. [Online]. Available: https://books.google.ca/books?id=Ve8eAQAAIAAJ

[20] R. Daendliker, "Concept of modes in optics and photonics," in *Sixth International Conference on Education and Training in Optics and Photonics*, J. J. Sanchez-Mondragon, Ed., vol. 3831, International Society for Optics and Photonics. SPIE, 2000, pp. 193 – 198. [Online]. Available: https://doi.org/10.1117/12.388718

[21] P. Sillard, M. Bigot-Astruc, and D. Molin, "Few-Mode Fibers for Mode-Division-Multiplexed Systems," *J. Lightwave Technol.*, vol. 32, no. 16, pp. 2824–2829, Aug 2014. [Online]. Available: http://jlt.osa.org/abstract.cfm?URI=jlt-32-16-2824

[22] T. Sakamoto, T. Mori, T. Yamamoto, and F. Yamamoto, "Few-mode fiber for optical MIMO transmission with low-computational complexity," *Proceedings of SPIE - The International Society for Optical Engineering*, vol. 8647, 01 2013.

[23] N. Iwai, N. Yokouchi, and A. Kasukawa, "850 nm VCSELs for 10 Gb/s operation," in *IEEE/LEOS Summer Topic All-Optical Networking: Existing and Emerging Architecture and Applications/Dynamic Enablers of Next-Generation Optical Communications Systems/Fast Optical Processing in Optical*, 2002, pp. WC2–WC2.

[24] S. A. Blokhin, J. A. Lott, N. N. Ledentsov, L. Y. Karachinsky, A. G. Kuzmenkov, I. I. Novikov, N. A. Maleev, G. Fiol, and D. Bimberg, "850 nm Optical Components for 25 Gb/s Optical Fiber Data Communication Links over 100 m at 85 °C," in *Optoelectronic Materials and Devices*. Optical Society of America, 2011, p. 830819. [Online]. Available: http://www.osapublishing.org/abstract.cfm?URI=ACP-2011-830819

[25] M. Chaciński, N. Chitica, S. Molin, N. Lalic, and O. Sahlén, "25.78 Gbps Data Transmission with 850 nm Multimode VCSEL Packaged in QSFP Form Factor Module," in *Optical Fiber Communication Conference/National Fiber Optic Engineers Conference 2013*. Optical Society of America, 2013, p. OW1B.1. [Online]. Available: http://www.osapublishing.org/abstract.cfm?URI=OFC-2013-OW1B.1

[26] J. Gustavsson, A. Larsson, Å. Haglund, J. Bengtsson, P. Westbergh, R. Safaisini, and E. Haglund, "High Speed 850nm VCSELs for $>$ 40 Gb/s Transmission," in *Optical Fiber Communication Conference/National Fiber Optic Engineers Conference 2013*. Optical Society of America, 2013, p. OTh4H.4. [Online]. Available: http://www.osapublishing.org/abstract.cfm?URI=OFC-2013-OTh4H.4

[27] D. M. Kuchta, C. L. Schow, A. V. Rylyakov, J. E. Proesel, F. E. Doany, C. Baks, B. H. Hamel-Bissell, C. Kocot, L. Graham, R. Johnson, G. Landry, E. Shaw, A. MacInnes, and J. Tatum, "A 56.1 Gb/s NRZ Modulated 850 nm VCSEL-Based Optical Link," in *Optical Fiber Communication Conference/National Fiber Optic*

Engineers Conference 2013. Optical Society of America, 2013, p. OW1B.5. [Online]. Available: http://www.osapublishing.org/abstract.cfm?URI=OFC-2013-OW1B.5

[28] J. A. Tatum, "The Evolution of 850 nm VCSELs from 10 Gb/s to 25 and 56 Gb/s," in *Optical Fiber Communication Conference*. Optical Society of America, 2014, p. Th3C.1. [Online]. Available: http://www.osapublishing.org/abstract.cfm?URI=OFC-2014-Th3C.1

[29] M. Nouri, H. Shahoie, T. LaFave, S. Ashrafi, and D. MacFarlane, "Orbital Angular Momentum Multiplexing using Low-Cost VCSELs for Datacenter Applications," in *Frontiers in Optics 2016*. Optical Society of America, 2016, p. FW5D.5. [Online]. Available: http://www.osapublishing.org/abstract.cfm?URI=FiO-2016-FW5D.5

[30] S. A. Gebrewold, A. Josten, B. Baeuerle, M. Stubenrauch, S. Eitel, and J. Leuthold, "PAM-8 108 Gbit/s transmission using an 850nm multi-mode VCSEL," in *The European Conference on Lasers and Electro-Optics*. Optical Society of America, 2017, p. CI_4_6.

[31] J. A. Tatum, G. D. Landry, D. Gazula, J. K. Wade, and P. Westbergh, "VCSEL-Based Optical Transceivers for Future Data Center Applications," in *Optical Fiber Communication Conference*. Optical Society of America, 2018, p. M3F.6. [Online]. Available: http://www.osapublishing.org/abstract.cfm?URI=OFC-2018-M3F.6

[32] L. M. Giovane, J. Wang, M. R. Murty, A. L. Harren, A.-N. Cheng, D. Dolfi, Z.-W. Feng, N. Leong, A. Sridhara, S.-J. Taslim, and J. Chu, "Development of Next Generation Data Communication VCSELs," in *Optical Fiber Communication Conference (OFC) 2020*. Optical Society of America, 2020, p. M3D.5. [Online]. Available: http://www.osapublishing.org/abstract.cfm?URI=OFC-2020-M3D.5

[33] A. Tarighat, R. C. J. Hsu, A. Shah, A. H. Sayed, and B. Jalali, "Fundamentals and challenges of optical multiple-input multiple-output multimode fiber links [Topics in Optical Communications]," *IEEE Communications Magazine*, vol. 45, no. 5, pp. 57–63, 2007.

[34] Y. Fazea and V. Mezhuyev, "Selective mode excitation techniques for mode-division multiplexing: A critical review," *Optical Fiber Technology*, vol. 45, pp. 280–288, 2018. [Online]. Available: https://www.sciencedirect.com/science/article/pii/S1068520018301536

[35] C. Zhong, X. Zhang, W. Hofmann, L. Yu, J. Liu, Y. Ning, and L. Wang, "Few-mode vertical-cavity surface-emitting laser: Optional emission of transverse modes with

different polarizations," *Applied Physics Express*, vol. 11, no. 5, p. 052702, apr 2018. [Online]. Available: https://doi.org/10.7567%2Fapex.11.052702

[36] A. Amphawan and Y. Fazea, "Laguerre-Gaussian mode division multiplexing in multimode fiber using SLMs in VCSEL arrays," *Journal of the European Optical Society-Rapid publications*, vol. 12, no. 1, pp. 1–11, 2016.

[37] B. Wang, W. V. Sorin, M. R. Tan, and S. Cheung, "Mode Division Multiplexing Using Vertical-Cavity Surface Emitting Lasers," Jun. 25 2020, US Patent App. 16/229,967.

[38] S. Kruk, F. Ferreira, N. Mac Suibhne, C. Tsekrekos, I. Kravchenko, A. Ellis, D. Neshev, S. Turitsyn, and Y. Kivshar, "Transparent Dielectric Metasurfaces for Spatial Mode Multiplexing," *Laser & Photonics Reviews*, vol. 12, no. 8, p. 1800031, 2018. [Online]. Available: https://onlinelibrary.wiley.com/doi/abs/10.1002/lpor.201800031

[39] Y.-Y. Xie, P.-N. Ni, Q.-H. Wang, Q. Kan, G. Briere, P.-P. Chen, Z.-Z. Zhao, A. Delga, H.-R. Ren, H.-D. Chen *et al.*, "Metasurface-integrated vertical cavity surface-emitting lasers for programmable directional lasing emissions," *Nat. Nanotechnol*, vol. 15, pp. 125–130, 2020.

[40] Zemax, "OpticStudio by Zemax," https://www.zemax.com/products/opticstudio, (Last accessed: October 15, 2020).

[41] ZEMAX, "Zemax Knowledgebase," https://my.zemax.com/en-US/Knowledge-Base/, (Last accessed: October 15, 2020).

[42] Edmund Optics, "Correct Material of IR applications," https://www.edmundoptics.com/knowledge-center/application-notes/optics/the-correct-material-for-infrared-applications/, (Last accessed: October 15, 2020).

[43] I. Manolis, J.-L. Bezy, A. Costantino, R. Vink, A. Deep, M. Ahmad, E. Amorim, M. Miranda, and R. Meynart, "The ESA RADGLASS activity: a radiation study of non rad-hard glasses," *Proceedings of SPIE - The International Society for Optical Engineering*, vol. 9639, pp. 96 391N–1, 10 2015.

[44] Finisar, "VCSEL modes," https://www.finisar.com/sites/default/files/downloads/application_note_vcsel_optical_modes.pdf, (Last accessed: October 15, 2020).

[45] H.-C. Kim and Y. H. Lee, "Hermite–Gaussian and Laguerre–Gaussian beams beyond the paraxial approximation," *Optics Communications*, vol. 169, no. 1, pp. 9 – 16, 1999. [Online]. Available: http://www.sciencedirect.com/science/article/pii/S0030401899004113

[46] A. Fardoost, H. Wen, H. Liu, F. G. Vanani, and G. Li, "Optimizing free space to few-mode fiber coupling efficiency," *Appl. Opt.*, vol. 58, no. 13, pp. D34–D38, May 2019. [Online]. Available: http://ao.osa.org/abstract.cfm?URI=ao-58-13-D34

[47] S. A. Akbari, A. Gholami, M. M. Rad, and Z. Mazaheri, "An optical subassembly model based on Silicon Optical Bench for VCSEL to MMF and PIN photodiode to MMF coupling," in *6th International Symposium on Telecommunications (IST)*, 2012, pp. 514–519.

[48] L. Samuel I-E, "Misalignment tolerance analysis of combined thick convex lens and lensed fiber scheme between vertical-cavity surface-emission lasers and single-model fibers," *Optical Engineering*, vol. 43, no. 9, pp. 2087 – 2099, 2004. [Online]. Available: https://doi.org/10.1117/1.1776186

[49] G. Ruffato, M. Massari, and F. Romanato, "Generation of high-order Laguerre Gaussian modes by means of spiral phase plates," *Opt. Lett.*, vol. 39, no. 17, pp. 5094–5097, Sep 2014. [Online]. Available: http://ol.osa.org/abstract.cfm?URI=ol-39-17-5094

[50] A. Amphawan, F. Payne, D. O'Brien, and N. Shah, "Derivation of an Analytical Expression for the Power Coupling Coefficient for Offset Launch Into Multimode Fiber," *Journal of Lightwave Technology*, vol. 28, no. 6, pp. 861–869, 2010.

[51] A. Gholami, Z. Toffano, A. Destrez, M. Pez, and F. Quentel, "Spatiotemporal and thermal analysis of VCSEL for short-range gigabit optical links," *Optical and quantum electronics*, vol. 38, no. 4-6, pp. 479–493, 2006.

[52] Thorlabs, "Selecting proper lens," https://www.thorlabs.com/tutorials.cfm?tabID=ba49b425-f85b-4549-8c1a-f111ddbb9099, (Last accessed: October 15, 2020).

[53] EdmundOptics, "Understanding optical lens geometry," https://www.edmundoptics.com/knowledge-center/application-notes/optics/understanding-optical-lens-geometries/, (Last accessed: October 15, 2020).

[54] N. Sheffi and D. Sadot, "Tilted Gaussian Beams Multiplexer for Graded-Index Multimode Fiber in Data-Centers Interconnections," *IEEE Photonics Journal*, vol. 7, no. 3, pp. 1–16, 2015.

[55] T. Wang, A. Yang, F. Shi, Y. Huang, J. Wen, and X. Zeng, "High-order mode lasing in all-FMF laser cavities," *Photon. Res.*, vol. 7, no. 1, pp. 42–49, Jan 2019. [Online]. Available: http://www.osapublishing.org/prj/abstract.cfm?URI=prj-7-1-42

[56] C. Yang, M. Wang, M. Tang, H. Wu, C. Zhao, T. Liu, S. Fu, and W. Tong, "Link optimized few-mode fiber Raman distributed temperature sensors," *Appl. Opt.*, vol. 57, no. 24, pp. 6923–6926, Aug 2018. [Online]. Available: http://ao.osa.org/abstract.cfm?URI=ao-57-24-6923

[57] B. Lee, "Review of the present status of optical fiber sensors," *Optical Fiber Technology*, vol. 9, no. 2, pp. 57 – 79, 2003. [Online]. Available: http://www.sciencedirect.com/science/article/pii/S1068520002005278

[58] E. Fearon, T. Sato, D. Wellburn, K. Watkins, and G. Dearden, "Thermal effects of substrate materials used in the laser curing of particulate silver inks," *Proceedings of the International Conference on Laser Assisted Net Shape Engineering*, vol. 5, 01 2007.

[59] R. Cox, D. Hayes, T. Chen, D. Ussery, D. Macfarlane, and E. Wilson, "Fabrication of micro-optics by microjet printing," *Proceedings of SPIE - The International Society for Optical Engineering*, vol. 2383, 05 1995.

[60] W. R. Cox, T. Chen, and D. J. Hayes, "Micro-optics fabrication by ink-jet printers," *Optics and Photonics News*, vol. 12, no. 6, pp. 32–35, 2001.

[61] SIJ Technology, "Super Inkjet Printer," https://sijtechnology.com/en/products/, (Last accessed: October 15, 2020).

[62] Epoxy Technologies, "EPO-TEK 353ND," http://www.epotek.com/site/administrator/components/com_products/assets/files/Style_Uploads/353ND.pdf, (Last accessed: October 15, 2020).

[63] G. Shi, L. Garfias, and W. Smyrl, "Preparation of a Gold-Sputtered Optical Fiber as a Microelectrode for Electrochemical Microscopy," *Journal of The Electrochemical Society*, vol. 145, pp. 2011–2016, 06 1998.